



Copyright Undertaking

This thesis is protected by copyright, with all rights reserved.

By reading and using the thesis, the reader understands and agrees to the following terms:

1. The reader will abide by the rules and legal ordinances governing copyright regarding the use of the thesis.
2. The reader will use the thesis for the purpose of research or private study only and not for distribution or further reproduction or any other purpose.
3. The reader agrees to indemnify and hold the University harmless from and against any loss, damage, cost, liability or expenses arising from copyright infringement or unauthorized usage.

IMPORTANT

If you have reasons to believe that any materials in this thesis are deemed not suitable to be distributed in this form, or a copyright owner having difficulty with the material being included in our database, please contact lbsys@polyu.edu.hk providing details. The Library will look into your claim and consider taking remedial action upon receipt of the written requests.

GLOBAL DYNAMICS AND SPATIAL
PATTERNS OF A RATIO-DEPENDENT
PREYTAXIS MODEL DRIVEN BY THE
ACCELERATION

MU SHUHAO

MPhil

The Hong Kong Polytechnic University

2023

The Hong Kong Polytechnic University
Department of Applied Mathematics

Global Dynamics and Spatial Patterns of a
Ratio-dependent Prey-taxis Model Driven by the
Acceleration

Mu Shuhao

A thesis submitted in partial fulfilment of the requirements
for the degree of Master of Philosophy

Dec. 2022

CERTIFICATE OF ORIGINALITY

I hereby declare that this thesis is my own work and that, to the best of my knowledge and belief, it reproduces no material previously published or written, nor material that has been accepted for the award of any other degree or diploma, except where due acknowledgement has been made in the text.

_____ (Signed)

_____ Mu Shuhao _____ (Name of student)

Abstract

The movement of individual organism has been recognized for a long time as a significant factor influencing the spatio-temporal distribution of populations. Numerous reaction-diffusion models that can track spatial and temporal changes in population size have been created to explain how the movement of individuals affects the spatial and temporal distribution of biological populations. Using these reaction-diffusion systems, variety of biological processes, such as reproduction or genetics, tumor growth, wound healing, patch production, etc., have been demonstrated. In these reaction-diffusion models, the dispersal strategy of individuals is typically assumed to be random diffusion; however, it cannot explain some of the more complex ecological processes involving rational movements (e.g., directed movements of dispersing individuals that are chemotaxis, preytaxis, etc. to increase their chances of survival) nor accurately reflect the non-Brownian movements of individuals. If diffusion is assumed to be only random, no spatially inhomogeneous patterns will be observed for the predator-prey system, which cannot explain the spatio-temporal heterogeneity of patterns observed in the experiment. Therefore, it is more reasonable to incorporate rational motion into the model in certain real-world circumstances. In this thesis, we study the celebrated predator-prey systems with preytaxis, where the taxis term representing the rational movement is formulated as an advection term.

Numerous investigations addressing predator-prey interactions have demonstrated that in some preytaxis models, it is more plausible to assume that the predator's

acceleration (rather than preytactic velocity) is proportional to the prey density gradient. Such acceleration-driven preytaxis models were introduced in [9, 39] to explain the observed spatial heterogeneity of predators and prey. This thesis is dedicated to exploring the global dynamics of a ratio-dependent preytaxis system driven by acceleration. The existence of classical solutions with uniform-in-time bound was established in any spatial dimension. Moreover, we prove the global stability of the spatially homogeneous prey-only and coexistence steady states under certain conditions on system parameters and show that the convergence rates are exponential type. For the system parameters outside the stability regime, linear stability analysis is performed to find the possible patterning regimes and numerical simulations are used to demonstrate that spatially inhomogeneous time-periodic patterns will typically arise which can interpret the spatial-temporal heterogeneity observed in experiments.

Key Words: Ratio-dependent; predator-prey; preytaxis; global stability; pattern formation.

Acknowledgements

First and foremost, I would like to express my deepest gratitude to my chief supervisor Prof. Zhian Wang for his detailed guidance, full support, strict regulation, and warm encouragement. His dedication and enthusiasm for research and life always motivate me to face the challenges and difficulties during my MPhil study. He taught me how to conduct academic research at the master's level, including finding topics, consulting literature, and how to write academic papers. Besides, he acted as a pioneer and leader on my research route, occasionally admonishing and advising me. Professor Wang's guidance centered not only on study and research but also on the human heart's core, which will benefit me throughout my life. Without his academic guidance and humanistic care, I cannot complete this thesis.

Next, I would like to extend my sincerest gratitude to Dr. Lou Yijun and Dr. He Daihai, who served as judges during my Confirmation of Registration. Their evaluation and encouragement are also crucial factors in my ability to successfully complete my MPhil studies.

Then, I want to appreciate the Department of Applied Mathematics for providing essential research support. The academic atmosphere is positive and active due to the cozy research environment. The abundance of online colloquiums and the numerous appropriate course planning options extend my vision and inspire me all the time.

Finally, I am grateful to my parents for their companies and supports. Undoubtedly, their unconditional support and unwavering confidence in me are the strongest

arms and the warmest harbor in my heart for helping me to keep the faith to complete the study.

Contents

Abstract	iv
Acknowledgements	vi
List of Figures	x
List of Notations	xi
1 Introduction	1
1.1 Biological interactions	1
1.2 ODE type predator-prey systems	2
1.3 PDE type predator-prey systems	4
1.4 The considered problem and main results	7
1.5 Organization of the thesis	9
2 Global boundedness	11
2.1 Preliminaries	11
2.2 Local existence	13
2.3 Uniform-in-time <i>a priori</i> estimates	16
2.4 Global boundedness	21
3 Global stability	22
3.1 Preliminaries	22
3.2 Global stability of the prey-only steady state	26
3.3 Global stability of the coexistence steady state	32

4	Spatially heterogeneous time-periodic patterns	36
4.1	Linear instability analysis	36
4.2	Spatio-temporal patterns	40
5	Conclusions and future plans	46
5.1	Conclusions	46
5.2	Future plans	47
	Bibliography	48

List of Figures

- 4.1 Numerical simulation of spatio-temporal patterns generated by (1.4.1) with $\gamma = 15$ in the interval $[0, 10]$, where the initial value (u_0, v_0, w_0) is given by (4.2.2) and other parameter values are chosen as in (4.2.1). 41
- 4.2 Numerical simulation of spatio-temporal patterns generated by (1.4.1) with $\gamma = 30$ in the interval $[0, 10]$, where the initial value (u_0, v_0, w_0) is given by (4.2.2) and other parameter values are chosen as in (4.2.1). 42
- 4.3 Numerical simulation of spatio-temporal patterns generated by (1.4.1) with $\gamma = 12.4872$ in the interval $[0, 10]$, where the initial value (u_0, v_0, w_0) is given by (4.2.2) and other parameter values are chosen as in (4.2.1). 43

List of Notations

Basic notations

\mathbb{N}	Natural numbers set $\{0, 1, 2, 3, \dots\}$.
\mathbb{N}_+	Positive natural numbers set $\{1, 2, 3, \dots\}$.
\mathbb{R}^n	n -dimensional Euclidean space with $n \in \mathbb{N}_+$
x	$x = (x_1, x_2, \dots, x_n) \in \mathbb{R}^n$ with $n \in \mathbb{N}_+$.

Derivatives

u_{x_i} $u_{x_i} = \frac{\partial u}{\partial x_i}(x) = \lim_{h \rightarrow 0} \frac{u(x+he_i) - u(x)}{h}$, provided this limit exists.

$u_{x_i x_j}$ $u_{x_i x_j} = \frac{\partial^2 u}{\partial x_i \partial x_j}$.

$D^\alpha u(x)$ For a multiindex $\alpha = (\alpha_1, \dots, \alpha_n)$ ($\alpha_i \in \mathbb{N}$),

$$D^\alpha u(x) = \frac{\partial^{|\alpha|} u(x)}{\partial x_1^{\alpha_1} \dots \partial x_n^{\alpha_n}} = \partial_{x_1}^{\alpha_1} \dots \partial_{x_n}^{\alpha_n} u,$$

where $|\alpha| = \alpha_1 + \dots + \alpha_n$.

$D^k u(x)$ $D^k u(x) = \{D^\alpha u(x) \mid |\alpha| = k\}$ for $k \in \mathbb{N}$.

$|D^k u|$ $|D^k u| = \left(\sum_{|\alpha|=k} |D^\alpha u|^2 \right)^{1/2}$

∇u $\nabla u = Du = (u_{x_1}, \dots, u_{x_n}) =$ gradient vector.

Δu $\Delta u = \sum_{i=1}^n u_{x_i x_i}$

$D^2 u$ $D^2 u = \begin{pmatrix} u_{x_1 x_1} & \dots & u_{x_1 x_n} \\ & \ddots & \\ u_{x_n x_1} & \dots & u_{x_n x_n} \end{pmatrix}_{n \times n}$.

Function Space

$C(\Omega)$	$\{u : \Omega \rightarrow \mathbb{R} \mid u \text{ is continuous}\}.$
$C(\bar{\Omega})$	$\{u \in C(\Omega) \mid u \text{ is uniformly continuous on bounded subsets of } \Omega\}.$
$C^k(\bar{\Omega})$	$\{u : \Omega \rightarrow \mathbb{R} \mid u \text{ has } k \text{ continuous derivatives}\}.$
$L^p(\Omega)$	$\{u : \Omega \rightarrow \mathbb{R} \mid u \text{ is Lebesgue measurable, } \ u\ _{L^p(\Omega)} < \infty\},$ where

$$\|u\|_{L^p(\Omega)} = \left(\int_{\Omega} |u|^p dx \right)^{\frac{1}{p}} \quad (1 \leq p < \infty).$$

$L^\infty(\Omega)$	$\{u : \Omega \rightarrow \mathbb{R} \mid u \text{ is Lebesgue measurable, } \ u\ _{L^\infty(\Omega)} < \infty\},$ where
--------------------	---

$$\|u\|_{L^\infty(\Omega)} = \text{ess sup}_{\Omega} |u|.$$

$L^p_{\text{loc}}(\Omega)$	$\{u : \Omega \rightarrow \mathbb{R} \mid u \in L^p(V) \text{ for each } V \subset\subset \Omega\}.$
$C^{k,\gamma}(\bar{\Omega})$	$\{u \in C^k(\bar{\Omega}) \mid \ u\ _{C^{k,\gamma}(\bar{\Omega})} < \infty\},$ where

$$\|u\|_{C^{k,\gamma}(\bar{\Omega})} = \sum_{|\alpha| \leq k} \|D^\alpha u\|_{C(\bar{\Omega})} + \sum_{|\alpha|=k} [D^\alpha u]_{C^{0,\gamma}(\bar{\Omega})}.$$

$W^{k,p}(\Omega)$	$\{u : \Omega \rightarrow \mathbb{R} \mid u \text{ is locally summable functions, } \ u\ _{W^{k,p}(\Omega)} < \infty\},$ where
-------------------	--

$$\|u\|_{W^{k,p}(\Omega)} = \begin{cases} \left(\sum_{|\alpha| \leq k} \int_{\Omega} |D^\alpha u|^p dx \right)^{1/p}, & 1 \leq p < \infty, \\ \sum_{|\alpha| \leq k} \text{ess sup}_{\Omega} |D^\alpha u|, & p = \infty. \end{cases}$$

Others

\mathbb{R}	Set of real numbers
\mathbb{R}^+	Set of positive real numbers
\mathbb{N}	Set of natural numbers
\mathbb{Z}	Set of integers

Chapter 1

Introduction

This dissertation investigates the global dynamics of a ratio-dependent predator-prey model with prey taxis driven by acceleration. The first result is the global existence of a unique classical bounded solution in any spatial dimension. Second, the global stability of the spatially homogeneous prey-only and coexistence steady states are established under certain conditions on system parameters. Linear analysis is performed to identify possible patterns, and numerical simulations are conducted to demonstrate that spatially inhomogeneous time-periodic patterns will typically emerge outside the stable parameter regimes. In this chapter, we first introduce the biological background of predation and then present the classical mathematical models (the predator-prey model) used to model the interaction between predators and prey, including ODE and PDE models.

1.1 Biological interactions

A biological interaction in ecology is the influence that two creatures living in the same community have on each other. If the interaction occurs within the same species, it is an intraspecific interaction; if the interaction occurs between different species, it is an interspecific interaction. There are three types of fundamental interactions in ecology, including mutualism (symbiosis), competition and predation. In

this thesis, our study focus on the classical predator-prey model describing predation interactions.

1.2 ODE type predator-prey systems

The ODE type predator-prey system typically takes the form of

$$\begin{cases} u_t = \alpha\beta uF(u, v) - uh_1(u), \\ v_t = h_2(v) - \beta uF(u, v), \\ u(0), v(0) > 0, \end{cases} \quad (1.2.1)$$

where $u(t)$ and $v(t)$ represent the population densities of the predator and the prey at time $t > 0$ respectively, $\beta uF(u, v)$ represents the interspecific interaction with the intrinsic predation rate $\beta > 0$, the constant $\alpha > 0$ denotes the conversion rate from prey to predator. $F(u, v)$ is called functional response function accounting for the intake rate of predators as a function of prey density, $h_1(u)$ and $h_2(v)$ are the predator mortality rate function and the prey growth function, respectively. The predator mortality rate function $h_1(u)$ is typically in the form of

$$h_1(u) = \theta_1 + \theta_2 u$$

with constants $\theta_1 > 0$ and $\theta_2 \geq 0$ denoting the natural death rate and density-dependent death (cf. [27]), respectively. The functional response function $F(u, v)$ and the prey growth function $h_2(v)$ typically take the forms of (cf. [43, 32])

$$F(u, v) = F(v) = \begin{cases} v \text{ (Lotka-Volterra type or Holling type I)}, \\ \frac{v}{\lambda+v} \text{ (Holling type II)}, \\ \frac{v^\kappa}{\lambda^\kappa+v^\kappa} \text{ (Holling type III)}, \end{cases} \quad (1.2.2)$$

and

$$h_2(v) = vf(v) = \begin{cases} \eta v \left(1 - \frac{v}{K}\right) \text{ (Logistic type)}, \\ \eta v \left(1 - \frac{v}{K}\right) \left(\frac{v}{L} - 1\right) \text{ (Allee effect type)}, \end{cases} \quad (1.2.3)$$

where the constants $\kappa > 1$, and $K, \lambda, \eta > 0$ stand for carrying capacity, half saturation constant, maximal predator growth rate, respectively.

In the case of $h_1(u) \equiv \theta_1 = \theta$, $F(u, v)$ is Holling type II and $h_2(v)$ is Logistic type, the model (1.2.1) turns into

$$\begin{cases} u_t = \frac{\alpha\beta uv}{\lambda+v} - \theta u, \\ v_t = \eta v \left(1 - \frac{v}{K}\right) - \frac{\beta uv}{\lambda+v}. \end{cases} \quad (1.2.4)$$

Denote

$$(u_*, v_*) = \left(\frac{\alpha\eta\lambda((\alpha\beta - \theta)K - \theta\lambda)}{K(\theta - \alpha\beta)^2}, \frac{\theta\lambda}{\alpha\beta - \theta} \right) \quad \text{for } \alpha\beta > \theta, K > \frac{\theta\lambda}{\alpha\beta - \theta}$$

by the positive constant equilibrium of (1.2.4), then the model possesses the famous “paradox of enrichment” (or called “biological control paradox”, cf. [19] and the references therein): u_* increases with K , however, v_* does not increase with K ; moreover, (u_*, v_*) is stable for small K but unstable for large K . This means that the model (1.2.4) can not describe some biological phenomena properly.

Various laboratory experiments and observations provide evidences that functional response function ought to depend on the densities of both prey and predators, especially when predators must search for food (and therefore must share or compete for food), i.e., $F(u, v) = F(v/u)$ (see [19, the second page] and [56, the first page]) with

$$F(v/u) = \frac{\frac{v}{u}}{m + \frac{v}{u}} = \frac{v}{mu + v} \quad \text{with some constant } m > 0. \quad (1.2.5)$$

The system (1.2.1) with $h_1(u) \equiv \theta_1 = \theta$ and the ratio-dependent functional response function (1.2.5) turns into

$$\begin{cases} u_t = \frac{\alpha\beta uv}{mu+v} - \theta u, \\ v_t = \eta v \left(1 - \frac{v}{K}\right) - \frac{\beta uv}{mu+v}, \\ u(0), v(0) > 0. \end{cases} \quad (1.2.6)$$

For the ratio-dependent predator-prey model (1.2.6), “paradox of enrichment” can not occur [25]. With the scaling

$$t \rightarrow \eta t, \quad v \rightarrow \frac{v}{K}, \quad u \rightarrow \frac{mu}{K}$$

the model (1.2.6) can be nondimensionalized into the form of Gause-type predator-prey system

$$\begin{cases} u_t = \delta u \left(\frac{v}{u+v} - r \right), \\ v_t = v \left(1 - v \right) - \frac{\mu uv}{u+v}, \\ u(0), v(0) > 0, \end{cases} \quad (1.2.7)$$

where

$$\delta = \frac{\alpha\beta}{\eta}, \quad r = \frac{\theta}{\alpha\beta}, \quad \mu = \frac{\beta}{m\eta}.$$

[19] obtained a complete classification of the asymptotic behavior of the solution to (1.2.7). When considering a constant harvesting effect, i.e., the second equation of (1.2.7) becomes

$$v_t = v \left(1 - v \right) - \frac{\mu uv}{u+v} - h$$

with a constant $h > 0$. [56], multiple kinds of bifurcations occurring for different parameters are proved.

1.3 PDE type predator-prey systems

To interpret the aggregation phenomenon observed in the field experiment designed to study the interactions between predators and prey under the area-restricted search strategy, Kareiva and Odell [24] proposed the following reaction-diffusion-advection model

$$\begin{cases} u_t = d_u \Delta u - \nabla \cdot (\chi(u, v) \nabla v) + G_1(u, v), \\ v_t = d_v \Delta v + G_2(u, v), \end{cases} \quad (1.3.1)$$

where $u(x, t)$ and $v(x, t)$ represent the population densities of the predator and the prey at position $x \in \Omega$ and time $t > 0$, respectively. The positive constant d_u is the predator diffusion coefficient and d_v is the prey's. The functions $G_1(u, v)$ and $G_2(u, v)$ describe the population interactions between the predator and the prey, taking the classical form of

$$G_1(u, v) = \alpha\beta uF(u, v) - uh_1(u), \quad G_2(u, v) = h_2(v) - \beta uF(u, v). \quad (1.3.2)$$

The advection term $-\nabla \cdot (\chi(u, v)\nabla v)$ represents the preytaxis with prey-tactic coefficient $\chi(u, v)$ which may depend on the predator or prey density. In model (1.3.1), a fundamental assumption is that the preytactic velocity is proportional to the prey density gradient. However, many observations reveal that it is more reasonable to assume that the individual acceleration (rather than the velocity itself) is proportional to the gradient of the stimulus. Typical examples of these observations exhibit that schooling fish adjust their acceleration according to the difference between ambient and preferred temperatures (cf. [37, 16]), the moving flea-beetles modify their acceleration in conformity with food patch quality (cf. [23]), the individual acceleration of the swarm of midges is determined by the distance from the center (cf. [34, 35]), and so on. For the purpose of mathematical analyses of phenomena of the predator acceleration adjusting in the light of the prey density gradient observed in Kareiva [23] and Winder *et al* [52], the following preytaxis model driven by acceleration was proposed in [9, 39]

$$\begin{cases} u_t = d_u\Delta u - \nabla \cdot (u\mathbf{w}) + G_1(u, v), \\ v_t = d_v\Delta v + G_2(u, v), \\ \mathbf{w}_t = d_w\Delta \mathbf{w} + \gamma\nabla v, \end{cases} \quad (1.3.3)$$

where u and v still denote the population densities of the predator and the prey respectively, and the vector-valued function \mathbf{w} is the velocity of the predator whose variation, denoted by \mathbf{w}_t , is proportional to the prey density gradient ∇v with the

coefficient $\gamma > 0$ as described by the third equation in (1.3.3) where the diffusion term $d_w \Delta \mathbf{w}$ is explained as a social equilibrium effect like intraspecific interactions (cf. [16]). The positive constants d_u, d_v, d_w are diffusion coefficients.

With different types of predator-prey interactions, there are plenty of results for the classical prey-taxis model (1.3.1), such as traveling waves [26], pattern formation [27, 13, 18, 28, 49], global stability [1, 2, 11, 42, 30, 21, 55, 45, 54, 44, 22], and so on. Compared to (1.3.1), the model (1.3.3) where the acceleration assumption is used has much fewer works. For different types of functional response functions, linear stability analyses are conducted and patterns are shown with numerical simulations, see [9] in a two dimensional parallelepiped box Ω and [39, 13] in an interval $\Omega = [0, L]$. Recently in [31], when the functional response function takes the form of $F(u, v) = F(v)$, the existence of global-in-time bounded classical solutions in a general bounded domain in any spatial dimensions is established, where the global stability of spatially homogeneous prey-only/coexistence steady states with decay rates is also investigated. Moreover, by applying linear stability analysis and performing numerical simulations, it is demonstrated in [31] that spatially inhomogeneous time-periodic patterns will typically arise for the certain parameters outside the stability regime.

Corresponding to the ODE type ratio-dependent predator-prey model (1.2.6), the PDE type ratio-dependent predator-prey model with prey-taxis proposed as (cf. [11])

$$\left\{ \begin{array}{ll} u_t = \Delta u - \nabla \cdot (\chi u \nabla v) + \frac{\alpha uv}{mu+v} - \mu u, & x \in \Omega, \quad t > 0, \\ v_t = d \Delta v - \frac{uv}{mu+v} + v f(v), & x \in \Omega, \quad t > 0, \\ \nabla u \cdot \mathbf{n} = \nabla v \cdot \mathbf{n} = 0, & x \in \partial\Omega, \quad t > 0, \\ u(x, 0) = u_0(x), \quad v(x, 0) = v_0(x), & x \in \Omega, \end{array} \right. \quad (1.3.4)$$

where $\Omega \subset \mathbb{R}^n$ ($n \in \mathbb{N}^+$) is a bounded domain with smooth boundary, \mathbf{n} is the unit outward normal vector on $\partial\Omega$, and d, χ, α, μ are positive constants. The

results for “non-preytaxis” case (i.e., (1.3.4) with $\chi = 0$) are plentiful including the (local) stability of both constant and non-constant steady states (cf. [36]), the global stability of homogeneous steady states (cf. [15]), the finite difference solution and its asymptotic behavior (cf. [50]), pattern formation and Hopf-Turing bifurcation (cf. [10, 40, 41, 47, 38]). For (1.3.4) with $\chi > 0$, in any dimensional bounded domain, the existence of global-in-time bounded solutions are established and the homogeneous steady states are proved to be exponentially stable in certain system parameters conditions (cf. [11]). The existence of non-constant steady state is also numerically showed in [11], which later proved in [12] in the case of Ω is a bounded interval.

1.4 The considered problem and main results

To the best of our knowledge, there is fewer result about the ratio-dependent preytaxis model driven by acceleration. The goal of this thesis is to explore the global dynamics of such models. Specifically, we shall consider the following system

$$\left\{ \begin{array}{ll} u_t = d_u \Delta u - \nabla \cdot (u \mathbf{w}) + \alpha u F(v/u) - \mu u, & x \in \Omega, \quad t > 0, \\ v_t = d_v \Delta v + v f(v) - u F(v/u), & x \in \Omega, \quad t > 0, \\ \mathbf{w}_t = d_w \Delta \mathbf{w} + \gamma \nabla v, & x \in \Omega, \quad t > 0, \\ \nabla u \cdot \mathbf{n} = \nabla v \cdot \mathbf{n} = 0, \quad \mathbf{w} = \mathbf{0}, & x \in \partial\Omega, \quad t > 0, \\ (u, v, \mathbf{w})(x, 0) = (u_0, v_0, \mathbf{w}_0)(x), & x \in \Omega, \end{array} \right. \quad (1.4.1)$$

where $F(v/u)$ is defined by (1.2.5), $\Omega \subset \mathbb{R}^n$ ($n \in \mathbb{N}^+$) is a bounded domain with smooth boundary, \mathbf{n} is the unit outward normal vector on $\partial\Omega$, and $d_u, d_v, d_w, \alpha, \mu, \gamma$ are positive constants. In this thesis, we shall only consider the logistic type. The function $f(v)$ is supposed to satisfy the following conditions (cf. [11]):

- (H) The function $f : [0, \infty) \rightarrow \mathbb{R}$ is continuously differentiable satisfying $f'(v) \leq -\delta$ for some constant $\delta > 0$ and for all $v \geq 0$, and there exists a positive constant K such that $f(0) > 0, f(K) = 0$ and $f(v) < 0$ for all $v > K$.

The first main theorem stated below asserts that the system (1.4.1) has a unique global-in-time classical solution which is uniform-in-time bounded.

Theorem 1.4.1. *Suppose that $n \geq 1$, $u_0, v_0 \gneq 0$ with $u_0, v_0 \in W^{1,\infty}(\Omega)$, $\mathbf{w}_0(x) \in (W^{1,\infty}(\Omega))^n$ and the hypothesis (H) hold. Then the system (1.4.1) has a unique global classical solution (u, v, \mathbf{w}) satisfying*

$$\begin{cases} u, v \in C(\bar{\Omega} \times [0, \infty)) \cap C^{2,1}(\bar{\Omega} \times (0, \infty)) & \text{with } u \geq 0, 0 \leq v \leq M, \\ \mathbf{w} \in (C(\bar{\Omega} \times [0, \infty)) \cap C^{2,1}(\bar{\Omega} \times (0, \infty)))^n, \end{cases}$$

where the positive constant M is defined by

$$M := \max \{ \|v_0\|_{L^\infty(\Omega)}, K \}. \quad (1.4.2)$$

Moreover, we have

$$\|u\|_{L^\infty(\Omega)} + \|v(\cdot, t)\|_{W^{1,\infty}(\Omega)} + \|\mathbf{w}(\cdot, t)\|_{W^{1,\infty}(\Omega)} \leq C \quad \text{for all } t > 0, \quad (1.4.3)$$

where $C > 0$ is a constant independent of time t .

We next focus on the global stability of homogeneous steady states. Except the extinction equilibrium $(0, 0, \mathbf{0})$, the system (1.4.1) has other two possible equilibria (u_s, v_s, \mathbf{w}_s) :

$$(u_s, v_s, \mathbf{w}_s) = \begin{cases} (0, K, \mathbf{0}), & \text{if } \alpha \leq \mu, \\ (0, K, \mathbf{0}), (u_*, v_*, \mathbf{0}), & \text{if } \alpha > \mu \quad \text{and} \quad f(0) > \frac{1}{m}, \end{cases} \quad (1.4.4)$$

where $(0, K, \mathbf{0})$ is the prey-only steady state and $(u_*, v_*, \mathbf{0})$ is the coexistence steady state with $u_*, v_* > 0$ which is determined by the following algebraic equations:

$$\mu = \frac{\alpha v_*}{m u_* + v_*} \quad \text{and} \quad f(v_*) = \frac{u_*}{m u_* + v_*}. \quad (1.4.5)$$

The constant steady states of \mathbf{w} is $\mathbf{0}$ since $\mathbf{w}|_{\partial\Omega} = \mathbf{0}$. Our following result is stated about asymptotic dynamics of (1.4.1).

Theorem 1.4.2. *Suppose that the conditions in Theorem 1.4.1 holds.*

- (i) *Assume that $\alpha \leq \mu$, then the prey-only steady state $(0, K, \mathbf{0})$ is globally asymptotically stable. Moreover, if $\alpha < \mu$, then $(0, K, \mathbf{0})$ is exponentially stable, i.e., there exist positive constants C , σ_1 and t_1 such that*

$$\|u\|_{L^\infty(\Omega)} + \|v - K\|_{L^\infty(\Omega)} + \|\mathbf{w}\|_{L^\infty(\Omega)} \leq Ce^{-\sigma_1 t} \quad \text{for all } t > t_1.$$

- (ii) *Assume that $\alpha > \mu$, (u_*, v_*) is given by (1.4.5) and $f^{-1}(\frac{1}{m}) > \frac{\alpha - \mu}{\delta\alpha}$. There exists a number $d_w^* > 0$ such that if $d_w > d_w^*$, then the coexistence steady state $(u_*, v_*, \mathbf{0})$ is globally exponentially stable, i.e., there exist positive constants C , σ_2 and t_2 such that*

$$\|u - u_*\|_{L^\infty(\Omega)} + \|v - v_*\|_{L^\infty(\Omega)} + \|\mathbf{w}\|_{L^\infty(\Omega)} \leq Ce^{-\sigma_2 t} \quad \text{for all } t > t_2.$$

Remark 1.4.1. In the case of $\alpha > \mu$, the condition $f^{-1}(\frac{1}{m}) > \frac{\alpha - \mu}{\delta\alpha}$ along with the hypothesis (H) implies that $f(0) > f(\frac{\alpha - \mu}{\delta\alpha}) > \frac{1}{m}$, which is satisfied the conditions in (1.4.4) for the emergence of the coexistence state.

1.5 Organization of the thesis

In this chapter, we have introduced the biological background of predation, and the mathematical models: predator-prey models (with preytaxis) describing this ecological interaction. By comparing the existing literature, we present our motivation and the problem which deserves to study. We focus on the global dynamics of a ratio-dependent preytaxis model driven by acceleration. Specifically, we shall investigate the global existence, global boundedness, global stability, and pattern formation of the model. To achieve this and present our results properly, this thesis is organized as the following.

Chapter 2 is devoted to establishing the global existence and boundedness of solutions to our problem. The main mathematical tools contains the well-known

parabolic regularities such as the L^p estimate, the Schauder estimate, and the L^p - L^q -estimates for the Dirichlet/Neumann heat semigroup, etc. Based on Amann's theorem the local existence of solutions and the corresponding extension criterion can be established. Then the key point is to derive appropriate uniform *a priori* estimates of solutions, by applying the extension criterion allows us to extend the local solutions to the global one's.

Once the global boundedness of solutions is established, we can study the global stability of constant equilibria in Chapter 3. To determine stable parameter regimes, we construct appropriate Lyapunov functionals and utilize compactness arguments. In addition, we will investigate the rate of convergence of solutions under particular parameter values.

Outside stable parameter regimes, the large-time behavior of solutions is obscure. In chapter 4, we conduct linear analysis to find the unstable parameter regimes and perform numerical simulations to exhibit possible patterns. We shall see that spatially heterogeneous time-periodic patterns will typically arise.

Finally, conclusions and future plans are discussed in chapter 5.

Chapter 2

Global boundedness

This chapter is devoted to establishing the global existence and boundedness (in the sense of $L^\infty(\Omega)$) of solutions to (1.4.1). There are three main steps towards this direction. First, we use the well-known parabolic regularities to establish the local existence of solutions and the corresponding extension criterion. Second, we shall derive the *a priori* estimates which are necessary to obtain the uniform boundedness of solutions. Finally, due to the obtained *a priori* estimates, we shall use the parabolic regularities (such as the L^p estimate, the Schauder estimate (cf. [29]) and the smooth properties of the Neumann/Dirichlet heat semigroup) to show the uniform-in-time boundedness of solutions with the extension criterion can achieve our goal. First of all, we give the following preparations.

2.1 Preliminaries

Before proceeding, we introduce some notations used throughout this thesis.

- Without confusion, we shall abbreviate $\int_0^t \int_\Omega f(\cdot, s) dx ds$ and $\int_\Omega f(\cdot, t) dx$ as $\int_0^t \int_\Omega f$ and $\int_\Omega f$ respectively.
- Unless specified, C and C_i ($i = 1, 2, 3, \dots$) denote generic positive constants which may vary line by line.

- We use C_P to denote the following Poincaré constant

$$C_P := \inf \left\{ C > 0 \left| \int_{\Omega} |\varphi|^2 \leq C \int_{\Omega} |\nabla \varphi|^2 \text{ for all } \varphi \in (W_0^{1,2}(\Omega))^n \right. \right\}. \quad (2.1.1)$$

In order to derive the *a priori* estimates for \mathbf{w} , we shall need the following L^p - L^q -estimates for the Dirichlet heat semigroup.

Lemma 2.1.1 (cf. [31, Lemma 2.4]). *Let $(e^{t\Delta})_{t \geq 0}$ be the Dirichlet heat semigroup in $\Omega \subset \mathbb{R}^n$ ($n \geq 1$), $\lambda_1 > 0$ denote the first nonzero eigenvalue of $-\Delta$ in Ω under the Dirichlet boundary condition. Then the following properties hold.*

- (i) *If $1 \leq q \leq p \leq \infty$, then for any $z \in L^q(\Omega)$, it holds that*

$$\|e^{t\Delta} z\|_{L^p(\Omega)} \leq C(1 + t^{-\frac{n}{2}(\frac{1}{q} - \frac{1}{p})})e^{-\lambda_1 t} \|z\|_{L^q(\Omega)} \quad \text{for all } t > 0$$

and

$$\|\nabla e^{t\Delta} z\|_{L^p(\Omega)} \leq C \left(1 + t^{-\frac{1}{2} - \frac{n}{2}(\frac{1}{q} - \frac{1}{p})}\right) e^{-\lambda_1 t} \|z\|_{L^q(\Omega)} \quad \text{for all } t > 0.$$

- (ii) *If $2 \leq p < \infty$, then for any $z \in W^{1,p}(\Omega)$, it holds that*

$$\|\nabla e^{t\Delta} z\|_{L^p(\Omega)} \leq C e^{-\lambda_1 t} \|\nabla z\|_{L^p(\Omega)} \quad \text{for all } t > 0.$$

- (iii) *If $1 < q \leq p \leq \infty$, then for $\mathbf{z} \in (L^q(\Omega))^n$, one has*

$$\|e^{t\Delta} \nabla \cdot \mathbf{z}\|_{L^p(\Omega)} \leq C(1 + t^{-\frac{1}{2} - \frac{n}{2}(\frac{1}{q} - \frac{1}{p})})e^{-\lambda_1 t} \|\mathbf{z}\|_{L^q(\Omega)} \quad \text{for all } t > 0.$$

Noting that u and v satisfy homogeneous Neumann boundary condition, we also need the following smooth properties Neumann heat semigroup.

Lemma 2.1.2 (cf. [53, Lemma 1.3]). *Let $(e^{t\Delta})_{t \geq 0}$ be the Neumann heat semigroup in Ω , and let $\lambda_2 > 0$ denote the first nonzero eigenvalue of $-\Delta$ in Ω under Neumann boundary conditions. Then the following properties hold.*

(i) If $1 \leq q \leq p \leq \infty$ then for all $z \in L^q(\Omega)$ satisfying $\int_{\Omega} z = 0$, it holds that

$$\|e^{t\Delta} z\|_{L^p(\Omega)} \leq C \left(1 + t^{-\frac{n}{2}(\frac{1}{q} - \frac{1}{p})}\right) e^{-\lambda_2 t} \|z\|_{L^q(\Omega)} \quad \text{for all } t > 0.$$

(ii) If $1 \leq q \leq p \leq \infty$ then for all $z \in L^q(\Omega)$, it holds that

$$\|\nabla e^{t\Delta} z\|_{L^p(\Omega)} \leq C \left(1 + t^{-\frac{1}{2} - \frac{n}{2}(\frac{1}{q} - \frac{1}{p})}\right) e^{-\lambda_2 t} \|z\|_{L^q(\Omega)} \quad \text{for all } t > 0.$$

(iii) If $2 \leq p < \infty$ then for all $z \in W^{1,p}(\Omega)$, it holds that

$$\|\nabla e^{t\Delta} z\|_{L^p(\Omega)} \leq C e^{-\lambda_2 t} \|\nabla z\|_{L^p(\Omega)} \quad \text{for all } t > 0.$$

(iv) Let $1 < q \leq p < \infty$. Then for all $\mathbf{z} \in (L^q(\Omega))^n$, it holds that

$$\|e^{t\Delta} \nabla \cdot \mathbf{z}\|_{L^p(\Omega)} \leq C \left(1 + t^{-\frac{1}{2} - \frac{n}{2}(\frac{1}{q} - \frac{1}{p})}\right) e^{-\lambda_2 t} \|\mathbf{z}\|_{L^q(\Omega)} \quad \text{for all } t > 0.$$

2.2 Local existence

For the first step, we shall establish the existence of local-in-time classical solutions.

Lemma 2.2.1. *Suppose that the conditions in Theorem 1.4.1 hold. Then there exists $T_{max} \in (0, \infty]$ such that (1.4.1) admits a unique classical solution (u, v, \mathbf{w}) on $[0, T_{max})$ satisfying*

$$\begin{cases} u, v \in C(\bar{\Omega} \times [0, T_{max})) \cap C^{2,1}(\bar{\Omega} \times (0, T_{max})), \\ \mathbf{w} \in [C(\bar{\Omega} \times [0, T_{max})) \cap C^{2,1}(\bar{\Omega} \times (0, T_{max}))]^n, \end{cases}$$

and

$$u > 0, \quad 0 < v \leq M \text{ in } \Omega \times (0, T_{max}), \quad (2.2.1)$$

where M is given by (1.4.2). Moreover,

$$\begin{cases} \text{either } T_{max} = \infty, \text{ or} \\ \lim_{t \rightarrow T_{max}} \sup (\|u(\cdot, t)\|_{L^\infty(\Omega)} + \|v(\cdot, t)\|_{L^\infty(\Omega)} + \|\mathbf{w}(\cdot, t)\|_{L^\infty(\Omega)}) = \infty. \end{cases} \quad (2.2.2)$$

Proof. The local existence of classical solutions to (1.4.1) and the extension criterion (2.2.2) can be established according to the standard arguments (cf. [51] for instance) based on the Amann's theorem of parabolic systems in [5, 6]. (2.2.1) can be proved by applying the strong maximum principle and the comparison principle. (cf. [11, Lemma 2.2]). For readers' convenience, we give a detailed proof here.

Let

$$\psi = (\psi_1, \psi_2, \dots, \psi_{n+2})^T = (u, v, \mathbf{w})^T = (u, v, w_1, w_2, \dots, w_n)^T$$

be a $(n+2)$ -dimensional vector-valued function, where \mathbf{K}^T denotes the transpose of a matrix \mathbf{K} . Denote $\mathbf{0}_{p \times q}$ be a p -by- q zero matrix with two positive integers p and q . Let

$$\xi_i = (-\psi_{i+2}, \mathbf{0}_{1 \times i}, -\psi_1, \mathbf{0}_{1 \times (n-i)}), \quad i = 1, 2, \dots, n,$$

be a $(n+2)$ -dimensional vector-valued function, and

$$\mathbf{D}_i = \begin{pmatrix} \xi_i \\ \mathbf{P}_{(n+1) \times (n+2)} \end{pmatrix}, \quad i = 1, \dots, n,$$

be a square matrix of order $(n+2)$, where all elements of the matrix $\mathbf{P}_{(n+1) \times (n+2)}$ are 0 except $(i+1)$ -by-2 element is γ . Then the system (1.4.1) can be rewritten as

$$\begin{cases} \psi_t = \mathbf{A} \cdot \Delta \psi + \sum_{i=1}^n \mathbf{D}_i \cdot \partial_i \psi + \mathbf{F}, & x \in \Omega, t > 0, \\ \mathcal{B} \psi = 0, & x \in \partial \Omega, t > 0, \\ \psi(\cdot, 0) = (u_0, v_0, \mathbf{w}_0), & x \in \Omega, \end{cases} \quad (2.2.3)$$

where

$$\mathbf{A} = \begin{pmatrix} d_u & 0 & 0 \\ 0 & d_v & 0 \\ 0 & 0 & d_w \mathbf{E}_n \end{pmatrix}$$

is a constant square matrix of order $(n+2)$ with \mathbf{E}_n being the identity matrix of

order n , and \mathbf{F} is a $(n + 2)$ -dimensional vector-valued function given by

$$\mathbf{F} = \begin{pmatrix} \frac{\alpha\psi_1\psi_2}{m\psi_1+\psi_2} - \mu\psi_1 \\ \psi_2 f(\psi_2) - \frac{\psi_1\psi_2}{m\psi_1+\psi_2} \\ \mathbf{0}_{n \times 1} \end{pmatrix}.$$

Moreover, the boundary operator \mathcal{B} is given by

$$\mathcal{B} = \begin{pmatrix} \partial_n & & \\ & \partial_n & \\ & & \mathbf{E}_n \end{pmatrix},$$

where ∂_n is the partial derivative with respect to \mathbf{n} .

Obviously, all eigenvalues of \mathbf{A} are positive, and hence the system (2.2.3) is uniform-in-time parabolic. The local existence and unique classical solutions follow from Amann's theorem [5, Theorem 7.3 and Corollary 9.3] and the blow-up criteria (2.2.2) follows from [6, Theorem 15.5].

The positivity of u follows from the strong maximum principle. To be precise, we rewrite the first equation of system (1.4.1) as follows

$$\begin{cases} u_t - d_u \Delta u + \mathbf{w} \cdot \nabla u + q(x, t)u = 0, & x \in \Omega, t \in (0, T_{max}), \\ \frac{\partial u}{\partial \mathbf{n}} = 0, & x \in \partial\Omega, t \in (0, T_{max}), \\ u(x, 0) = u_0 \geq 0 (\neq 0), & x \in \Omega, \end{cases}$$

where $q(x, t) = \nabla \cdot \mathbf{w} - \frac{\alpha v}{mu+v} + \mu$. By the maximum principle, we know that $u \geq 0$ in $\Omega \times (0, T_{max})$. Similarly, one can show that $v \geq 0$ in $\Omega \times (0, T_{max})$. Finally, it remains to prove $v \leq M$. Using the fact that u, v and $F(v/u)$ are non-negative, we have

$$\begin{cases} v_t - d_v \Delta v = f(v) - uF(v/u) \leq f(v), & x \in \Omega, t \in (0, T_{max}), \\ \frac{\partial v}{\partial \mathbf{n}} = 0, & x \in \partial\Omega, t \in (0, T_{max}), \\ v(x, 0) = v_0, & x \in \Omega. \end{cases} \quad (2.2.4)$$

Let $v^*(t)$ be a solution of the following ODE problem

$$\begin{cases} \frac{dv^*(t)}{dt} = v^*(t)f(v^*(t)), & t > 0, \\ v^*(0) = \|v_0\|_{L^\infty(\Omega)}. \end{cases} \quad (2.2.5)$$

Then the hypothesis (H) gives $v^*(t) \leq M = \max\{\|v_0\|_{L^\infty(\Omega)}, K\}$. Furthermore $v^*(t)$ is an upper solution of the following PDE problem

$$\begin{cases} V_t - d\Delta V = Vf(V), & x \in \Omega, t > 0, \\ \partial_{\mathbf{n}}V = 0, & x \in \partial\Omega, t > 0, \\ V(x, 0) = v_0(x), & x \in \Omega. \end{cases} \quad (2.2.6)$$

Therefore we have

$$0 < V(x, t) \leq v^*(t), \quad \text{for all } (x, t) \in \bar{\Omega} \times (0, \infty). \quad (2.2.7)$$

From (2.2.4)-(2.2.7), By the comparison principle, we have

$$0 < v(x, t) \leq V(x, t) \leq v^*(t) \leq M, \quad \text{for all } (x, t) \in \bar{\Omega} \times (0, T_{max}).$$

Therefore, (2.2.1) is proved, and the proof is completed. \square

2.3 Uniform-in-time *a priori* estimates

With the local existence obtained above, we are now in the position to derive the uniform-in-time *a priori* estimates for the local-in-time solutions. Suppose that the conditions in Theorem 1.4.1 hold and (u, v, \mathbf{w}) is the local-in-time classical solution to (1.4.1) with the maximum existing time $T_{max} \in (0, \infty]$. First, we have the following uniform-in-time L^1 -estimate for u .

Lemma 2.3.1. *There exists a constant $C > 0$ independent of t such that*

$$\|u(\cdot, t)\|_{L^1(\Omega)} \leq C \quad \text{for all } t \in (0, T_{max}).$$

Proof. Integrating the first equation in (1.4.1) over Ω with the boundary conditions in (1.4.1), and then using (1.2.5) and (2.2.1), we have

$$\frac{d}{dt} \int_{\Omega} u + \mu \int_{\Omega} u = \frac{\alpha uv}{mu + v} \leq \frac{\alpha M}{m} \quad \text{for all } t \in (0, T_{max}),$$

the proof is concluded by integrating the aforementioned ordinary differential equation with respect to t . \square

We now derive the L^∞ -estimate for \mathbf{w} , which is a direct consequence of the L^p - L^q -estimates for the Dirichlet heat semigroup stated in Lemma 2.1.1.

Lemma 2.3.2. *For all $t \in (0, T_{max})$, there exists a constant $C > 0$ independent of $t > 0$ such that*

$$\|\mathbf{w}(\cdot, t)\|_{L^\infty(\Omega)} \leq C. \quad (2.3.1)$$

Proof. By Duhamel's principle, one has

$$\begin{aligned} \mathbf{w}(t) &= e^{d_w t \Delta} \mathbf{w}_0 + \gamma \int_0^t e^{d_w(t-s)\Delta} \nabla v(\cdot, s) ds, \\ &= e^{d_w t \Delta} \mathbf{w}_0 + \gamma \int_0^t \nabla e^{d_w(t-s)\Delta} v(\cdot, s) ds \quad \text{for all } t \in (0, T_{max}). \end{aligned} \quad (2.3.2)$$

By Lemma 2.1.1, we have

$$\begin{aligned} \|\mathbf{w}(\cdot, t)\|_{L^\infty(\Omega)} &\leq C \|\mathbf{w}_0\|_{L^\infty(\Omega)} + C \int_0^t (1 + (t-s)^{-\frac{1}{2}}) e^{-\lambda_1(t-s)} \|v(\cdot, s)\|_{L^\infty(\Omega)} ds \\ &\leq C \|\mathbf{w}_0\|_{L^\infty(\Omega)} + C \int_0^t (1 + (t-s)^{-\frac{1}{2}}) e^{-\lambda_1(t-s)} ds \\ &\leq C \quad \text{for all } t \in (0, T_{max}). \end{aligned} \quad (2.3.3)$$

The proof is completed. \square

We can proceed to derive *a priori* L^∞ -estimate of u .

Lemma 2.3.3. *There exists a constant $C > 0$ independent of $t > 0$ such that*

$$\|u(\cdot, t)\|_{L^\infty(\Omega)} \leq C \quad \text{for all } t \in (0, T_{max}). \quad (2.3.4)$$

Proof. Multiplying the first equation of (1.4.1) by pu^{p-1} with $p > 1$, integrating by parts, using (2.2.1) and $\frac{v}{mu+v} \leq 1$, one has

$$\begin{aligned} & \frac{d}{dt} \int_{\Omega} u^p + p\mu \int_{\Omega} u^p + d_u(p-1) \frac{4}{p} \int_{\Omega} |\nabla u^{\frac{p}{2}}|^2 \\ &= p(p-1) \int_{\Omega} u^{p-1} \mathbf{w} \cdot \nabla u + \alpha p \int_{\Omega} \frac{u^p v}{mu+v} \\ &\leq 2(p-1) \int_{\Omega} u^{\frac{p}{2}} \mathbf{w} \cdot \nabla u^{\frac{p}{2}} + \alpha p \int_{\Omega} u^p \quad \text{for all } t \in (0, T_{max}), \end{aligned} \quad (2.3.5)$$

By Lemma 2.3.2 and Young's inequality, we have

$$2(p-1) \int_{\Omega} u^{\frac{p}{2}} \mathbf{w} \cdot \nabla u^{\frac{p}{2}} \leq d_u(p-1) \frac{2}{p} \int_{\Omega} |\nabla u^{\frac{p}{2}}|^2 + 2C_1 \frac{p(p-1)}{d_u} \int_{\Omega} u^p \quad (2.3.6)$$

for all $t \in (0, T_{max})$, which substituted into (2.3.5) yields

$$\frac{d}{dt} \int_{\Omega} u^p + p\mu \int_{\Omega} u^p + \frac{2d_u(p-1)}{p} \int_{\Omega} |\nabla u^{\frac{p}{2}}|^2 \leq \left(2C_1 \frac{p(p-1)}{d_u} + \alpha p \right) \int_{\Omega} u^p \quad (2.3.7)$$

for all $t \in (0, T_{max})$. By Lemma 2.3.1 and the Gagliardo-Nirenberg inequality we know that

$$\begin{aligned} \int_{\Omega} u^p &= \|u^{\frac{p}{2}}\|_{L^2(\Omega)}^2 \leq C \left(\|\nabla u^{\frac{p}{2}}\|_{L^2(\Omega)}^{2\theta} \|u^{\frac{p}{2}}\|_{L^{\frac{2}{p}}(\Omega)}^{2(1-\theta)} + \|u^{\frac{p}{2}}\|_{L^{\frac{2}{p}}(\Omega)}^2 \right) \\ &\leq C \|\nabla u^{\frac{p}{2}}\|_{L^2(\Omega)}^{2\theta} + C \quad \text{for all } t \in (0, T_{max}), \end{aligned} \quad (2.3.8)$$

where

$$\theta = \frac{\frac{p}{2} - \frac{1}{2}}{\frac{1}{n} + \frac{p}{2} - \frac{1}{2}} \in (0, 1).$$

Since $\theta \in (0, 1)$, it follows from Young's inequality that

$$\left(2C_1 \frac{p(p-1)}{d_u} + \alpha p \right) \int_{\Omega} u^p \leq \frac{d_u(p-1)}{p} \int_{\Omega} |\nabla u^{\frac{p}{2}}|^2 + C(p) \quad (2.3.9)$$

for all $t \in (0, T_{max})$. Substituting this inequality into (2.3.7) gives

$$\frac{d}{dt} \int_{\Omega} u^p + p\mu \int_{\Omega} u^p + \frac{d_u(p-1)}{p} \int_{\Omega} |\nabla u^{\frac{p}{2}}|^2 \leq C(p) \quad \text{for all } t \in (0, T_{max}). \quad (2.3.10)$$

Solving the above ordinary differential inequality, we get

$$\|u(\cdot, t)\|_{L^p(\Omega)} \leq C(p) \quad \text{for all } t \in (0, T_{max}).$$

Taking $p = 2n$, we have

$$\|u(\cdot, t)\|_{L^{2n}(\Omega)} \leq C \quad \text{for all } t \in (0, T_{max}).$$

By Duhamel's principle, one has

$$u(\cdot, t) = e^{d_u t \Delta} u_0 - \int_0^t e^{d_u(t-s)\Delta} \nabla \cdot (u \mathbf{w}) ds + \int_0^t e^{d_u(t-s)\Delta} \varphi(u, v) ds \quad \text{for all } t \in (0, T_{max}),$$

where $\varphi(u, v) = f(v) - \alpha u F(v/u)$. By Lemma 2.1.2, we have

$$\begin{aligned} \|u(\cdot, t)\|_{L^\infty(\Omega)} &\leq C \|u_0\|_{L^\infty(\Omega)} + C \int_0^t (1 + (t-s)^{-\frac{1}{2} - \frac{n}{2} \cdot \frac{1}{2n}}) e^{-\lambda_2(t-s)} \|u\|_{L^{2n}(\Omega)} \|\mathbf{w}\|_{L^\infty(\Omega)} ds \\ &\quad + C \int_0^t (1 + (t-s)^{-\frac{n}{2} \cdot \frac{1}{2n}}) e^{-\lambda_2(t-s)} \|\varphi(u, v)\|_{L^{2n}(\Omega)} ds \\ &\leq C \|u_0\|_{L^\infty(\Omega)} + C \int_0^t (1 + (t-s)^{-\frac{3}{4}}) e^{-\lambda_2(t-s)} ds \\ &\quad + C \int_0^t (1 + (t-s)^{-\frac{1}{4}}) e^{-\lambda_2(t-s)} ds \\ &\leq C \quad \text{for all } t \in (0, T_{max}). \end{aligned} \quad (2.3.11)$$

The proof is completed. \square

We now derive *a priori* L^∞ -estimate involving the gradient of v and \mathbf{w} .

Lemma 2.3.4. *There exists a constant $C > 0$ independent of $t > 0$ such that*

$$\|v(\cdot, t)\|_{W^{1,\infty}(\Omega)} + \|\mathbf{w}(\cdot, t)\|_{W^{1,\infty}(\Omega)} \leq C \quad \text{for all } t \in (0, T_{max}). \quad (2.3.12)$$

Proof. In view of Lemma 2.3.2 and Lemma 2.3.3, we only need to prove

$$\|\nabla v(\cdot, t)\|_{L^\infty(\Omega)} + \|\nabla \mathbf{w}(\cdot, t)\|_{L^\infty(\Omega)} \leq C \quad \text{for all } t \in (0, T_{max}). \quad (2.3.13)$$

Using the variation of constants representation of v we have

$$v(\cdot, t) = e^{d_v t \Delta} v_0 + \int_0^t e^{d_v(t-s)\Delta} \varphi(u(\cdot, s), v(\cdot, s)) ds \quad \text{for all } t \in (0, T_{max}),$$

where $\varphi(u, v) = f(v) - uF(v/u)$. It follows from the hypothesis (H), Lemma 2.3.3 and $F(v/u) \leq 1$ that

$$\begin{aligned} \|\varphi(u(\cdot, t), v(\cdot, t))\|_{L^\infty(\Omega)} &\leq \max_{v \in [0, m]} f(v) + \|uF(v/u)\|_{L^\infty(\Omega)} \\ &\leq \max_{v \in [0, m]} f(v) + \|u\|_{L^\infty(\Omega)} \\ &\leq C \quad \text{for all } t \in (0, T_{max}), \end{aligned}$$

which together with the L^p - L^q -estimates for the Neumann heat semigroup given in Lemma 2.1.2 shows that

$$\begin{aligned} \|\nabla v(\cdot, t)\|_{L^\infty(\Omega)} &\leq C \|v_0\|_{W^{1,\infty}(\Omega)} + C \int_0^t (1 + (t-s)^{-\frac{1}{2}}) e^{-\lambda_2(t-s)} \|\varphi\|_{L^\infty(\Omega)} ds \\ &\leq C \|v_0\|_{W^{1,\infty}(\Omega)} + C \int_0^t (1 + (t-s)^{-\frac{1}{2}}) e^{-\lambda_2(t-s)} ds \\ &\leq C \quad \text{for all } t \in (0, T_{max}). \end{aligned} \quad (2.3.14)$$

Similarly, via the variation of constants formula of w_i ($i = 1, 2, \dots, n$), we have

$$\nabla w_i(t) = \nabla e^{d_w t \Delta} w_i(\cdot, 0) + \gamma \int_0^t \nabla e^{d_w(t-s)\Delta} \partial_{x_i} v(\cdot, s) ds \quad (2.3.15)$$

for all $t \in (0, T_{max})$. By Lemma 2.1.1, for $i = 1, 2, \dots, n$, we have

$$\begin{aligned} \|\nabla w_i(\cdot, t)\|_{L^\infty(\Omega)} &\leq C \|w_i(\cdot, 0)\|_{W^{1,\infty}(\Omega)} + C \int_0^t (1 + (t-s)^{-\frac{1}{2}}) e^{-\lambda_1(t-s)} \|\nabla v(\cdot, s)\|_{L^\infty(\Omega)} ds \\ &\leq C \|w_i(\cdot, 0)\|_{W^{1,\infty}(\Omega)} + C \int_0^t (1 + (t-s)^{-\frac{1}{2}}) e^{-\lambda_1(t-s)} ds \\ &\leq C \quad \text{for all } t \in (0, T_{max}). \end{aligned} \quad (2.3.16)$$

This along with (2.3.14) proves (2.3.13). \square

2.4 Global boundedness

With the above uniform-in-time *a priori* estimates, we can prove Theorem 1.4.1.

Proof of Theorem 1.4.1. In view of the extension criterion (2.2.2), Lemma 2.3.3 and Lemma 2.3.4 first imply $T_{max} = \infty$, and then gives (1.4.2) and (1.4.3). \square

Chapter 3

Global stability

In this chapter, we investigate the large time behavior of solutions to the system (1.4.1) by constructing appropriate Lyapunov functionals and using compactness arguments. Specifically, we shall focus on the global stability of the prey-only steady state $(0, K, \mathbf{0})$ and the coexistence steady state $(u_*, v_*, \mathbf{0})$ (noting that it is easy to show the trivial steady state $(0, 0, \mathbf{0})$ is linearly unstable). Throughout this chapter, we suppose that the conditions in Theorem 1.4.1 hold and (u, v, \mathbf{w}) is the global classical solution of (1.4.1) obtained in Theorem 1.4.1. To begin with, we give the following preparations.

3.1 Preliminaries

Based on a bootstrap argument, we can obtain the following higher-order estimates of solutions for all $t \in [1, \infty)$.

Lemma 3.1.1. *Let (u, v, \mathbf{w}) be the unique global classical solution of (1.4.1), which is given by Theorem 1.4.1. Then for any fixed $0 < \theta < 1$, there exists $C(\theta) > 0$ such that*

$$\|u, v, \mathbf{w}\|_{C^{2+\theta, 1+\frac{\theta}{2}}(\bar{\Omega} \times [1, \infty))} \leq C(\theta). \quad (3.1.1)$$

Proof. This proof is based on a standard argument based on the regularities for parabolic equations (see [46, Theorem 2.1] for instance). For readers' convenience,

we sketch the proof below. The system (1.4.1) can be rewritten as

$$\begin{cases} u_t - d_u \Delta u + \mathbf{w} \cdot \nabla u = H_1(u, v, \mathbf{w}), & x \in \Omega, t > 0, \\ v_t = d_v \Delta v + H_2(u, v), & x \in \Omega, t > 0, \\ \mathbf{w}_t = d_w \Delta \mathbf{w} + \gamma \nabla v, & x \in \Omega, t > 0, \\ \nabla u \cdot \mathbf{n} = \nabla v \cdot \mathbf{n} = 0, \mathbf{w} = \mathbf{0}, & x \in \partial\Omega, t > 0, \\ u(x, 0) = u_0(x), v(x, 0) = v_0(x) \mathbf{w}(x, 0) = \mathbf{w}_0(x), & x \in \Omega, \end{cases} \quad (3.1.2)$$

where

$$\begin{cases} H_1(u, v, \mathbf{w}) = -u \nabla \cdot \mathbf{w} + \alpha u F(v/u) - \mu u, \\ H_2(u, v) = v f(v) - u F(v/u). \end{cases}$$

It follows from (1.4.3) that

$$\|\nabla v\|_{L^\infty(\Omega \times (0, \infty))} + \|H_1(u, v, \mathbf{w})\|_{L^\infty(\Omega \times (0, \infty))} + \|H_2(u, v)\|_{L^\infty(\Omega \times (0, \infty))} \leq C.$$

Now let $p \geq 1$ be a constant, we apply the interior L^p estimate [29, Theorems 7.30 and 7.35] to (3.1.2) to obtain

$$\|u\|_{W_p^{2,1}(\Omega \times [\frac{1}{2}, \infty))} + \|v\|_{W_p^{2,1}(\Omega \times [\frac{1}{2}, \infty))} + \|\mathbf{w}\|_{W_p^{2,1}(\Omega \times [\frac{1}{2}, \infty))} \leq C.$$

For appropriate large p , the Sobolev embedding theorem indicates that there is a positive constant $\theta \in (0, 1)$ such that

$$\|u\|_{C^{1+\theta, \frac{1+\theta}{2}}(\bar{\Omega} \times [\frac{1}{2}, \infty))} + \|v\|_{C^{1+\theta, \frac{1+\theta}{2}}(\bar{\Omega} \times [\frac{1}{2}, \infty))} + \|\mathbf{w}\|_{C^{1+\theta, \frac{1+\theta}{2}}(\bar{\Omega} \times [\frac{1}{2}, \infty))} \leq C,$$

which gives

$$\|\nabla v\|_{C^{\theta, \frac{\theta}{2}}(\bar{\Omega} \times [\frac{1}{2}, \infty))} + \|H_1(u, v, \mathbf{w})\|_{C^{\theta, \frac{\theta}{2}}(\bar{\Omega} \times [\frac{1}{2}, \infty))} + \|H_2(u, v)\|_{C^{\theta, \frac{\theta}{2}}(\bar{\Omega} \times [\frac{1}{2}, \infty))} \leq C.$$

This along with an application of the interior Schauder estimate (cf. [29]) to (3.1.2) proves (3.1.1) □

To proceed, we recall the following two basic results which plays a key role in deriving the global stability. Along with the constructed Lyapunov functionals can first show that $(u - u_s, v - v_s, \mathbf{w} - \mathbf{w}_s)$ convergence $(0, 0, \mathbf{0})$ in the $L^2(\Omega)$ norm, then obtain the global stability by a compactness argument.

Lemma 3.1.2. (cf. [48, Lemma 1.1]) *Let $\tau \geq 0, c > 0$ be constants, $\psi(t) \geq 0, \int_{\tau}^{\infty} \rho(t)dt < \infty$. Assume that $\varphi \in C^1([\tau, \infty))$, φ is bounded from below and satisfies*

$$\varphi'(t) \leq -c\psi(t) + \rho(t) \quad \text{in } [\tau, \infty).$$

If either $\psi \in C^1([\tau, \infty))$ and $\psi'(t) \leq k$ in $[\tau, \infty)$ for some $k > 0$, or $\psi \in C^\theta([\tau, \infty))$ and $\|\psi\|_{C^\theta([\tau, \infty))} \leq k$ for some constants $0 < \theta < 1$ and $k > 0$, then

$$\lim_{t \rightarrow \infty} \psi(t) = 0.$$

Lemma 3.1.3 (cf. [21, Lemma 4.1]). *For constant $\omega > 0$, we define*

$$\zeta(v) = v - \omega - \omega \ln \frac{v}{\omega},$$

which is a convex function such that $\zeta(v) \geq 0$. If $v \rightarrow \omega$ as $t \rightarrow \infty$, then there exists a constant $T > 0$ such that

$$\frac{1}{4\omega}(v - \omega)^2 \leq \zeta(v) = v - \omega - \omega \ln \frac{v}{\omega} \leq \frac{1}{\omega}(v - \omega)^2 \quad \text{for all } t \geq T.$$

We also recall the following lower bound for v .

Lemma 3.1.4 (cf. [11, Lemma 3.2]). *If $f(0) > \frac{1}{m}$ and the hypothesis (H) hold, then there are positive constants $\rho_0 > 0$ and $T > 0$ such that the solution (u, v, \mathbf{w}) of (1.4.1) satisfies*

$$v(x, t) \geq \rho_0 \quad \text{for all } (x, t) \in \bar{\Omega} \times (T, \infty) \tag{3.1.3}$$

and

$$\liminf_{t \rightarrow \infty} v(x, t) \geq \tilde{v} := f^{-1}\left(\frac{1}{m}\right) \quad \text{for all } x \in \bar{\Omega}. \tag{3.1.4}$$

Proof. The model studied in [11] is (1.3.4), which is different from the model (1.4.1). However, the parabolic equations satisfied by v of these two models are same. Hence, the comparison principle used in the proof of [11, Lemma 3.2] is also applicable here. For the sake of the integrity of this thesis, we shall cite the proof here.

Clearly, $F(s)/s = \frac{1}{(m+s)} \leq \frac{1}{m}$ for all $s \geq 0$. An application of the maximum principle to the second equation of (1.4.1) implies that there is a $0 < t_0 < \infty$ such that $\min_{x \in \bar{\Omega}} v(x, t_0) = \bar{v} > 0$ for all $x \in \Omega$. Considering the problem

$$\begin{cases} v_t - d\Delta v = v \left(f(v) - \frac{F(v/u)}{v/u} \right) \geq v \left(f(v) - \frac{1}{m} \right), & x \in \Omega, t > t_0, \\ \partial_\nu v = 0, & x \in \partial\Omega, t > t_0, \\ v(x, t_0) = \bar{v}, & x \in \Omega. \end{cases} \quad (3.1.5)$$

We denote $v_*(t)$ by the solution of the ODE problem

$$\begin{cases} \frac{dv_*(t)}{dt} = v_*(t) \left(f(v_*(t)) - \frac{1}{m} \right), & t > t_0, \\ v_*(t_0) = \bar{v} > 0. \end{cases} \quad (3.1.6)$$

Then the hypothesis (H) yields that $v_*(t) \geq \min\{\bar{v}, \tilde{v}\} =: \varrho$ for all $t \geq t_0$. It is obvious that $v_*(t)$ is a lower solution of the following PDE problem

$$\begin{cases} V_t^0 - d\Delta V^0 = V^0 \left(f(V^0) - \frac{1}{m} \right), & x \in \Omega, t > t_0, \\ \partial_\nu V^0 = 0, & x \in \partial\Omega, t > t_0, \\ V^0(x, t_0) = v(x, t_0), & x \in \Omega. \end{cases} \quad (3.1.7)$$

Then we have

$$v_*(t) \leq V^0(x, t) \text{ for all } (x, t) \in \bar{\Omega} \times (t_0, \infty). \quad (3.1.8)$$

Combining (3.1.5), (3.1.7) and (3.1.8), and using the comparison principle, we have

$$\varrho \leq v_*(t) \leq V^0(x, t) \leq v(x, t) \quad \text{for all } (x, t) \in \bar{\Omega} \times (t_0, \infty), \quad (3.1.9)$$

which gives (3.1.3). By Lemma 3.1, we note that $v(f(v) - 1/m) > 0$ for all $0 < v < \tilde{v}$.

Therefore from (3.1.6), we have

$$\liminf_{t \rightarrow \infty} v_*(t) \geq \tilde{v},$$

which along with (3.1.9) gives (3.1.4). \square

3.2 Global stability of the prey-only steady state

After the above preparations, we can now constructing suitable the Lyapunov functional for the prey-only steady state $(0, K, \mathbf{0})$. To begin with, we define two positive constants as the following

$$\Gamma_1 := \frac{\gamma^2 M^2 C_P}{d_w d_v K} \quad \text{and} \quad \Gamma_2 := \frac{\Gamma_1}{\mu m \delta \rho_0}, \quad (3.2.1)$$

where M , C_P , δ and ρ_0 are given by (1.4.2), (2.1.1), the hypothesis (H) and Lemma 3.1.4, respectively.

Lemma 3.2.1. *Assume that $\alpha \leq \mu$, the conditions in Theorem 1.4.1 hold, and the positive constants Γ_1 and Γ_2 are given by (3.2.1). Then the energy functional*

$$\mathcal{E}_1(t) := \Gamma_1 \int_{\Omega} \left(v - K - K \ln \frac{v}{K} \right) + (1 + \Gamma_2) \int_{\Omega} u + \int_{\Omega} |\mathbf{w}|^2 \quad \text{for all } t > 0 \quad (3.2.2)$$

satisfies

$$\frac{d}{dt} \mathcal{E}_1(t) \leq -\varepsilon_1 \int_{\Omega} \left((v - K)^2 + |\mathbf{w}|^2 \right) - (\mu - \alpha) \int_{\Omega} u \quad \text{for all } t > T_1, \quad (3.2.3)$$

where ε_1 and T_1 are two positive constants.

Proof. Using $\alpha \leq \mu$, $F(v/u) = \frac{v}{mu+v} \leq 1$, (2.2.1) and integrating the first equation of (1.4.1) over Ω along with the boundary condition $\nabla u \cdot \mathbf{n} |_{\partial\Omega} = \mathbf{w} |_{\partial\Omega} = \mathbf{0}$, we have

$$\begin{aligned} (1 + \Gamma_2) \frac{d}{dt} \int_{\Omega} u &= \int_{\Omega} (\alpha F(v/u) - \mu) u + \Gamma_2 \int_{\Omega} (\alpha v - \mu(mu + v)) \frac{u}{mu + v} \\ &\leq (\alpha - \mu) \int_{\Omega} u - \mu m \Gamma_2 \int_{\Omega} \frac{u^2}{mu + v} \quad \text{for all } t > 0. \end{aligned} \quad (3.2.4)$$

By the hypothesis (H) we have $f'(v) \leq -\delta$ for all $v \geq 0$, which along with (2.2.1), $f(K) = 0$, Young's inequality and the mean value theorem implies that

$$\begin{aligned}
& \frac{d}{dt} \int_{\Omega} \left(v - K - K \ln \frac{v}{K} \right) ds \\
&= -d_v K \int_{\Omega} \frac{|\nabla v|^2}{v^2} + \int_{\Omega} (v - K)(f(v) - f(K)) - \int_{\Omega} (v - K) \frac{u}{mu + v} \\
&\leq -\frac{d_v K}{M^2} \int_{\Omega} |\nabla v|^2 + f'(\xi) \int_{\Omega} (v - K)^2 - \int_{\Omega} (v - K) \frac{u}{mu + v} \\
&\leq -\frac{d_v K}{M^2} \int_{\Omega} |\nabla v|^2 - \delta \int_{\Omega} (v - K)^2 - \int_{\Omega} (v - K) \frac{u}{mu + v} \\
&\leq -\frac{d_v K}{M^2} \int_{\Omega} |\nabla v|^2 - \frac{\delta}{2} \int_{\Omega} (v - K)^2 + \frac{1}{2\delta} \int_{\Omega} \frac{u^2}{(mu + v)^2} \tag{3.2.5}
\end{aligned}$$

for all $t > 0$, where ξ between v and K is a positive constant. Multiplying the third equation of (1.4.1) by \mathbf{w} , integrating the resulting equation over Ω alongside the boundary condition $\mathbf{w}|_{\partial\Omega} = \mathbf{0}$, and using (2.1.1), we arrive at

$$\begin{aligned}
\frac{d}{dt} \int_{\Omega} |\mathbf{w}|^2 &= -2d_w \int_{\Omega} |\nabla \mathbf{w}|^2 + 2\gamma \int_{\Omega} \mathbf{w} \cdot \nabla v \\
&\leq -\frac{2d_w}{C_P} \int_{\Omega} |\mathbf{w}|^2 + 2\gamma \int_{\Omega} \mathbf{w} \cdot \nabla v \quad \text{for all } t > 0. \tag{3.2.6}
\end{aligned}$$

The combination of (3.2.2) and (3.2.4)-(3.2.6) implies that

$$\begin{aligned}
\frac{d}{dt} \mathcal{E}_1(t) &\leq (\alpha - \mu) \int_{\Omega} u - \frac{\delta \Gamma_1}{2} \int_{\Omega} (v - K)^2 - \frac{d_v K \Gamma_1}{M^2} \int_{\Omega} |\nabla v|^2 \\
&\quad - \frac{2d_w}{C_P} \int_{\Omega} |\mathbf{w}|^2 + 2\gamma \int_{\Omega} \mathbf{w} \cdot \nabla v \\
&\quad - \underbrace{\mu m \Gamma_2 \int_{\Omega} \frac{u^2}{mu + v} + \frac{\Gamma_1}{2\delta} \int_{\Omega} \frac{u^2}{(mu + v)^2}}_{=: I_1} \quad \text{for all } t > 0. \tag{3.2.7}
\end{aligned}$$

By (2.2.1), (3.2.1) and Lemma 3.1.4 we can find some $T_1 > 0$ such that

$$\begin{aligned} I_1 &= -\Gamma_1 \int_{\Omega} \frac{u^2}{(mu+v)^2} \left(\frac{mu+v}{\delta\rho_0} - \frac{1}{2\delta} \right) \\ &\leq -\Gamma_1 \int_{\Omega} \frac{u^2}{(mu+v)^2} \left(\frac{1}{\delta} - \frac{1}{2\delta} \right) \leq 0 \quad \text{for all } t > T_1. \end{aligned}$$

Hence (3.2.7) implies that

$$\frac{d}{dt} \mathcal{E}_1(t) \leq -(\mu - \alpha) \int_{\Omega} u - \frac{\delta\Gamma_1}{2} \int_{\Omega} (v - K)^2 - \int_{\Omega} \mathbf{Y}_1 \mathbf{X}_1 \mathbf{Y}_1^T \quad \text{for all } t > T_1, \quad (3.2.8)$$

where $\mathbf{Y}_1 := (\nabla v, \mathbf{w})$ and \mathbf{X}_1 is the matrix denoted by

$$\mathbf{X}_1 := \begin{pmatrix} \frac{d_v K \Gamma_1}{M^2} & -\gamma \\ -\gamma & \frac{2d_w}{C_P} \end{pmatrix}.$$

It is obvious that $\frac{d_v K \Gamma_1}{M^2} > 0$ and

$$|\mathbf{X}_1| := \begin{vmatrix} \frac{d_v K \Gamma_1}{M^2} & -\gamma \\ -\gamma & \frac{2d_w}{C_P} \end{vmatrix} = \frac{2d_w d_v K \Gamma_1}{M^2 C_P} - \gamma^2 = \gamma^2 > 0$$

due to (3.2.1). Based on the Sylvester's criterion, the matrix \mathbf{X}_1 is positive definite.

Thus, we can find a constant $\beta_1 > 0$ such that

$$\mathbf{Y}_1 \mathbf{X}_1 \mathbf{Y}_1^T \geq \beta_1 |\mathbf{Y}_1|^2. \quad (3.2.9)$$

Therefore, a combination of (3.2.8)-(3.2.9) shows that

$$\frac{d}{dt} \mathcal{E}_1(t) \leq -(\mu - \alpha) \int_{\Omega} u - \frac{\delta\Gamma_1}{2} \int_{\Omega} (v - K)^2 - \beta_1 \int_{\Omega} (|\nabla v|^2 + |\mathbf{w}|^2) \quad \text{for all } t > T_1,$$

which proves (3.2.3) by letting $\varepsilon_1 := \min \left\{ \beta_1, \frac{\delta\Gamma_1}{2} \right\}$. \square

We are now in the position to prove the following convergence property.

Lemma 3.2.2. *Suppose that the conditions in Lemma 3.2.1 hold, then for any $0 < \theta < 1$ we have*

$$\|u\|_{C^{2+\theta}(\bar{\Omega})} + \|v - K\|_{C^{2+\theta}(\bar{\Omega})} + \|\mathbf{w}\|_{C^{2+\theta}(\bar{\Omega})} \rightarrow 0 \quad \text{as } t \rightarrow \infty. \quad (3.2.10)$$

Proof. With Lemma 3.1.1 and Lemma 3.2.1, the proof of (3.2.10) can be followed from similar arguments as in [46, Lemma 3.4]. For the convenience of readers, we shall outline the proof here. Let $\mathcal{E}_1(t)$ be given by Lemma 3.2.1 and define

$$\mathcal{F}_1(t) := \int_{\Omega} ((v - K)^2 + |\mathbf{w}|^2) \quad \text{for all } t > 0.$$

Let $\theta \in (0, 1)$ be fixed, by (3.1.1) we have $\mathcal{E}_1(t) \in C^1([1, \infty))$, $\mathcal{F}_1(t) \geq 0$, $\mathcal{F}_1(t) \in C^\theta([1, \infty))$ and $\|\mathcal{F}_1\|_{C^\theta([1, \infty))} \leq C_1$ for some $C_1 > 0$. Next we prove that $\mathcal{E}_1(t)$ is bounded from below in $(0, \infty)$. Indeed, denoting

$$\psi(s) := s - K - K \ln \frac{s}{K} \quad \text{for } s > 0,$$

then we have $\psi(K) = \psi'(K) = 0$ and $\psi''(s) = \frac{K}{s^2} > 0$ for $s > 0$. Moreover, by Taylor's expansion, for any $s > 0$, we can find a number C_s between s and K such that

$$\psi(s) = \psi(K) + \psi'(K)(s - K) + \psi''(C_s)(s - K)^2 = \frac{K(s - K)^2}{C_s^2} \geq 0,$$

which along with (3.2.2) implies that $\mathcal{E}_1(t) \geq 0$ for all $t \in (0, \infty)$. Then we are in a position to apply Lemma 3.1.2 to (3.2.3) to obtain

$$\lim_{t \rightarrow \infty} (\mathcal{F}_1(t) + (\mu - \alpha)\|u_1\|_{L^1(\Omega)}) = 0.$$

Therefore,

$$\lim_{t \rightarrow \infty} (\|\mathbf{w}\|_{L^2(\Omega)} + \|v - K\|_{L^2(\Omega)} + (\mu - \alpha)\|u\|_{L^1(\Omega)}) = 0.$$

Taking $\theta' \in (0, 1)$ such that $0 < \theta < \theta' < 1$, then Lemma 3.1.1 indicates that

$$\|u, v, \mathbf{w}\|_{C^{2+\theta', 1+\frac{\theta'}{2}}(\bar{\Omega} \times [1, \infty))} \leq C(\theta'),$$

which alongside the compact arguments and the uniqueness of limits (cf. [46, (3.12)], see also [20, Remark 6.2]) shows that

$$\lim_{t \rightarrow \infty} (\|\mathbf{w}\|_{C^{2+\theta}(\bar{\Omega})} + \|v - K\|_{C^{2+\theta}(\bar{\Omega})} + (\mu - \alpha)\|u\|_{C^{2+\theta}(\bar{\Omega})}) = 0. \quad (3.2.11)$$

If $\alpha < \mu$, then (3.2.10) is a direct consequence of (3.2.11). If $\alpha = \mu$, in view of (3.2.11), it remains to prove that

$$\|u\|_{C^{2+\theta}(\bar{\Omega})} \rightarrow 0 \text{ as } t \rightarrow \infty. \quad (3.2.12)$$

By the second equation of (1.4.1), (1.4.5) and $f(K) = 0$, we obtain

$$\begin{aligned} \frac{d}{dt} \left(\frac{1}{|\Omega|} \int_{\Omega} v dx \right) &= \bar{v}'(t) = \frac{1}{|\Omega|} \int_{\Omega} [vf(v) - \alpha uF(v/u)] dx \\ &= \frac{1}{|\Omega|} \int_{\Omega} v (f(v) - f(K)) dx - \frac{\alpha}{|\Omega|} \int_{\Omega} uF(v/u) dx \\ &=: J_1(t) + J_2(t) \quad \text{for all } t > 0, \end{aligned} \quad (3.2.13)$$

where $\bar{\varphi} := \frac{1}{|\Omega|} \int_{\Omega} \varphi dx$ for $\varphi \in L^1(\Omega)$. It follows from the mean value theorem, the hypothesis (H), (3.2.11) and Hölder's inequality that $J_1(t) \rightarrow 0$ as $t \rightarrow \infty$ since

$$0 \leq |J_1(t)| \leq C \|v(\cdot, t)\|_{L^\infty(\Omega)} \int_{\Omega} |f'(\xi)| \cdot |v - K| \leq C \|v - K\|_{L^2(\Omega)} \max_{s \in [0, K]} |f'(s)| \rightarrow 0$$

as $t \rightarrow \infty$, where ξ is a constant between v and K . By (3.1.1) we know that

$$\|\bar{v}'\|_{C^{\theta/2}([1, \infty))} \leq C_2(\theta) \quad \forall 0 < \theta < 1,$$

which together with (3.2.11) shows that $\bar{v}'(t) \rightarrow 0$ as $t \rightarrow \infty$. Therefore, we can infer from (3.2.13) and $J_1(t) \rightarrow 0$ as $t \rightarrow \infty$ that $J_2(t) \rightarrow 0$ as $t \rightarrow \infty$. Using (1.4.3) and Lemma 3.1.4, we can find some $T_1 > 0$ such that

$$\frac{1}{F(v/u)} = \frac{mu + v}{v} \leq 1 + \frac{m\|u\|_{L^\infty(\Omega)}}{\rho_0} =: C_2 \quad \text{for all } t > T_1,$$

which implies that

$$0 \leq \int_{\Omega} u = \int_{\Omega} u \frac{F(v/u)}{F(v/u)} dx \leq C_2 \int_{\Omega} u F(v/u) = \frac{|\Omega|}{\alpha} C_2 |J_2| \rightarrow 0 \quad \text{as } t \rightarrow \infty.$$

Therefore, in the case of $\alpha = \mu$, we have proved that

$$\|u\|_{L^1(\Omega)} \rightarrow 0 \quad \text{as } t \rightarrow \infty. \quad (3.2.14)$$

With (3.2.14), by the compact arguments and the uniqueness of limits again, we can prove (3.2.12) and complete the proof. \square

In the case of $\alpha < \mu$, we can prove that the prey-only steady state is exponentially stable.

Lemma 3.2.3. *Suppose that the conditions in Lemma 3.2.1 hold. Then there exist positive constants C , σ_1 and t_1 such that*

$$\|u\|_{L^\infty(\Omega)} + \|v - K\|_{L^\infty(\Omega)} + \|\mathbf{w}\|_{L^\infty(\Omega)} \leq C e^{-\sigma_1 t} \quad \text{for all } t > t_1.$$

Proof. Using Lemma 3.1.3 and (3.2.10), we can find $t_1 > 1$ such that

$$\begin{aligned} \frac{1}{4K} \int_{\Omega} (v - K)^2 &\leq \int_{\Omega} \left(v - K - K \ln \frac{v}{K} \right) ds \\ &\leq \frac{1}{K} \int_{\Omega} (v - K)^2 \quad \text{for all } t > t_1. \end{aligned} \quad (3.2.15)$$

By $\alpha < \mu$, (3.2.3) and (3.2.15), we can find two positive constants C_1 and C_2 such that

$$\mathcal{E}'_1(t) \leq -C_1 \int_{\Omega} (u + (v - K)^2 + |\mathbf{w}|^2) \leq -C_2 \mathcal{E}_1(t) \quad \text{for all } t > t_1,$$

which implies that

$$\mathcal{E}_1(t) \leq \mathcal{E}_1(0) e^{-C_2 t} \quad \text{for all } t > t_1.$$

This together with the definition of $\mathcal{E}_1(t)$ and (3.2.15) shows that

$$\|u\|_{L^1(\Omega)} + \|\mathbf{w}\|_{L^2(\Omega)}^2 + \|v - K\|_{L^2(\Omega)}^2 \leq C_3 e^{-C_2 t} \quad \text{for all } t > t_1. \quad (3.2.16)$$

We shall extend this result to the estimates of L^∞ -norm. Indeed, (3.1.1) with $t_1 > 1$ implies that

$$\|u, v, \mathbf{w}\|_{W^{1,\infty}(\Omega)} \leq C \quad \text{for all } t \geq t_1,$$

which along with (3.2.16) and the Gagliardo-Nirenberg inequality

$$\begin{cases} \|\psi\|_{L^\infty(\Omega)} \leq C \|\psi\|_{W^{1,\infty}(\Omega)}^{\frac{n}{n+1}} \|\psi\|_{L^1(\Omega)}^{\frac{1}{n+1}}, \\ \|\psi\|_{L^\infty(\Omega)} \leq C \|\psi\|_{W^{1,\infty}(\Omega)}^{\frac{n}{n+2}} \|\psi\|_{L^2(\Omega)}^{\frac{2}{n+2}}, \end{cases} \quad \forall \psi \in W^{1,\infty}(\Omega) \quad (3.2.17)$$

completes the proof by letting $\sigma_1 := -\frac{C_2}{n+2}$. \square

Proof of Theorem 1.4.2 (i). Clearly, Theorem 1.4.2 (i) is a direct consequence of Lemma 3.2.2 and Lemma 3.2.3. \square

3.3 Global stability of the coexistence steady state

We next consider the stability of the coexistence steady state $(u_*, v_*, \mathbf{0})$ in the case of $\alpha > \mu$. Define two positive constants

$$\Gamma_3 := \alpha \frac{u_*}{v_*} = \frac{\alpha(\alpha - \mu)}{\mu m} \quad \text{and} \quad d_w^* := \frac{1}{8d_u d_v \alpha u_*} (\alpha d_v C_P u_*^2 + 4\gamma^2 C_P M^2 d_u), \quad (3.3.1)$$

where M , (u_*, v_*) and C_P are given by (1.4.2), (1.4.5) and (2.1.1), respectively.

Lemma 3.3.1. *Assume that $\alpha > \mu$, the conditions in Theorem 1.4.1 hold, and the positive constants Γ_3 and d_w^* are defined by (3.3.1). If*

$$d_w > d_w^* \quad \text{and} \quad \tilde{v} := f^{-1}(1/m) > \frac{\alpha - \mu}{\delta \alpha}, \quad (3.3.2)$$

then for all $t > 0$, the energy functional

$$\mathcal{E}_2(t) = \int_{\Omega} \left(u - u_* - u_* \ln \frac{u}{u_*} \right) + \Gamma_3 \int_{\Omega} \left(v - v_* - v_* \ln \frac{v}{v_*} \right) + \int_{\Omega} |\mathbf{w}|^2$$

satisfies

$$\frac{d}{dt} \mathcal{E}_2(t) \leq -\varepsilon_2 \int_{\Omega} \left((u - u_*)^2 + (v - v_*)^2 + |\mathbf{w}|^2 \right) \quad \text{for all } t > T_2, \quad (3.3.3)$$

where (u_*, v_*) is given by (1.4.5) and ε_2, T_2 are two positive constants..

Proof. Using the first equality in (1.4.5), for all $t > 0$, we have

$$\begin{aligned}
& \frac{d}{dt} \int_{\Omega} \left(u - u_* - u_* \ln \frac{u}{u_*} \right) \\
&= -d_u u_* \int_{\Omega} \frac{|\nabla u|^2}{u^2} + u_* \int_{\Omega} \mathbf{w} \cdot \frac{\nabla u}{u} + \int_{\Omega} (\alpha F(v/u) - \mu) (u - u_*) \\
&= -d_u u_* \int_{\Omega} \frac{|\nabla u|^2}{u^2} + u_* \int_{\Omega} \mathbf{w} \cdot \frac{\nabla u}{u} + \alpha \int_{\Omega} (F(v/u) - F(v_*/u_*)) (u - u_*). \quad (3.3.4)
\end{aligned}$$

Similarly as in deriving (3.2.5), it follows from the second equality in (1.4.5) and (2.2.1) that

$$\begin{aligned}
& \frac{d}{dt} \int_{\Omega} \left(v - v_* - v_* \ln \frac{v}{v_*} \right) \\
&= -d_v v_* \int_{\Omega} \frac{|\nabla v|^2}{v^2} + \int_{\Omega} (v - v_*) \left(f(v) - \frac{u}{mu + v} \right) \\
&= -d_v v_* \int_{\Omega} \frac{|\nabla v|^2}{v^2} + \int_{\Omega} (v - v_*) (f(v) - f(v_*)) + \int_{\Omega} \left(\frac{u_*}{mu_* + v_*} - \frac{u}{mu + v} \right) (v - v_*) \\
&\leq -\frac{d_v v_*}{M^2} \int_{\Omega} |\nabla v|^2 - \delta \int_{\Omega} (v - v_*)^2 + \int_{\Omega} \left(\frac{u_*}{mu_* + v_*} - \frac{u}{mu + v} \right) (v - v_*) \quad (3.3.5)
\end{aligned}$$

for all $t > 0$, where we have used the mean value theorem along with the hypothesis (H) in the last inequality. Then the combination on (3.2.6), (3.3.4) and (3.3.5) shows that

$$\frac{d}{dt} \mathcal{E}_2(t) \leq -\delta \Gamma_3 \int_{\Omega} (v - v_*)^2 - \int_{\Omega} \mathbf{Y}_2 \mathbf{X}_2 \mathbf{Y}_2^T + I_2 \quad \text{for all } t > 0, \quad (3.3.6)$$

where for all $t > 0$, $\mathbf{Y}_2 := \left(\frac{\nabla u}{u}, \nabla v, \mathbf{w} \right)$, \mathbf{X}_2 is the matrix denoted by

$$\mathbf{X}_2 := \begin{pmatrix} d_u u_* & 0 & -\frac{u_*}{2} \\ 0 & \frac{d_v v_* \Gamma_3}{M^2} & -\gamma \\ -\frac{u_*}{2} & -\gamma & \frac{2d_w}{C_P} \end{pmatrix},$$

and

$$I_2 := \alpha \int_{\Omega} (F(v/u) - F(v_*/u_*)) (u - u_*) + \Gamma_3 \int_{\Omega} \left(\frac{u_*}{mu_* + v_*} - \frac{u}{mu + v} \right) (v - v_*).$$

It is obvious that $d_u u_* > 0$, $\frac{1}{M^2} d_u d_v u_* v_* \Gamma_3 > 0$ and

$$\begin{aligned} |\mathbf{X}_2| &:= \begin{vmatrix} d_u u_* & 0 & -\frac{u_*}{2} \\ 0 & \frac{d_v v_* \Gamma_3}{M^2} & -\gamma \\ -\frac{u_*}{2} & -\gamma & \frac{2d_w}{C_P} \end{vmatrix} \\ &= \frac{u_*}{4C_P M^2} (8d_u d_v d_w \alpha u_* - \alpha d_v C_P u_*^2 - 4\gamma^2 C_P M^2 d_u) > 0 \end{aligned}$$

due to (3.3.2). Based on the Sylvester's criterion, the matrix \mathbf{X}_2 is positive definite and we can find a constant $\beta_2 > 0$ such that

$$\mathbf{Y}_2 \mathbf{X}_2 \mathbf{Y}_2^T \geq \beta_2 |\mathbf{Y}_2|^2. \quad (3.3.7)$$

For I_2 , direct calculations along with $(\alpha u_* - \Gamma_3 v_*) = 0$ show that

$$\begin{aligned} I_2 &= \frac{m}{(mu_* + v_*)} \int_{\Omega} \frac{vu_* - uv_*}{mu + v} (\alpha(u - u_*) + \Gamma_3(v - v_*)) \\ &= \frac{m}{(mu_* + v_*)} \int_{\Omega} \frac{1}{mu + v} (-\alpha v_*(u - u_*)^2 + u_* \Gamma_3 (v - v_*)^2) \quad \text{for all } t > 0, \end{aligned}$$

which alongside (1.4.3), (3.3.6) and (3.3.7) implies that

$$\begin{aligned} \frac{d}{dt} \mathcal{E}_2(t) &\leq -\delta \Gamma_3 \int_{\Omega} (v - v_*)^2 - \beta_2 \int_{\Omega} |\mathbf{w}|^2 - C_1 \int_{\Omega} (u - u_*)^2 + \frac{mu_* \Gamma_3}{(mu_* + v_*)} \int_{\Omega} \frac{(v - v_*)^2}{mu + v} \\ &\leq -\beta_2 \int_{\Omega} |\mathbf{w}|^2 - C_1 \int_{\Omega} (u - u_*)^2 - \Gamma_3 \int_{\Omega} \psi(v)(v - v_*)^2 \end{aligned} \quad (3.3.8)$$

for all $t > 0$, where $\psi(v) := \delta - \frac{mu_*}{v(mu_* + v_*)}$. We next prove that $\psi(v)$ has a positive lower bound for sufficient large t . Indeed, it follows from the second inequality in (3.3.2) that $\varepsilon_0 := \tilde{v} - \frac{\alpha - \mu}{\delta \alpha} > 0$, which along with (3.1.4) implies that there exists $T_2 > 0$ such that

$$v(x, t) \geq \tilde{v} - \frac{\varepsilon_0}{2} = \frac{1}{2} \left(\tilde{v} + \frac{\alpha - \mu}{\delta \alpha} \right) > 0 \quad \text{for all } t > T_2.$$

Therefore, denoting $\beta_3 := \frac{2mu_*}{(\tilde{v} + \frac{\alpha - \mu}{\delta \alpha})(mu_* + v_*)}$, using $1 + \frac{v_*}{mu_*} = \frac{\alpha}{\alpha - \mu}$ (due to (1.4.5)) and the second inequality in (3.3.2), we have

$$\psi(v) \geq \delta - \beta_3 = \frac{\beta_3}{2} \left(\frac{\alpha \delta \tilde{v}}{\alpha - \mu} - 1 \right) =: \beta_4 > 0 \quad \text{for all } t > T_2. \quad (3.3.9)$$

Letting $\varepsilon_2 := \min \{C_1, \beta_2, \beta_4 \Gamma_3\}$ and making use of (3.3.8) and (3.3.9), we get (3.3.3) and complete the proof. \square

With the same arguments for Lemma 3.2.2 and Lemma 3.2.3, we arrive at the following conclusion and omit the proof for brevity.

Lemma 3.3.2. *Suppose that the conditions in Lemma 3.3.1 hold, then for any $0 < \theta < 1$ we have*

$$\|u - u_*\|_{C^{2+\theta}(\bar{\Omega})} + \|v - v_*\|_{C^{2+\theta}(\bar{\Omega})} + \|\mathbf{w}\|_{C^{2+\theta}(\bar{\Omega})} \rightarrow 0 \quad \text{as } t \rightarrow \infty.$$

Lemma 3.3.3. *Suppose that the conditions in Lemma 3.3.1 hold, Then there exist positive constants C , σ_2 and t_2 such that*

$$\|u - u_*\|_{L^\infty(\Omega)} + \|v - v_*\|_{L^\infty(\Omega)} + \|\mathbf{w}\|_{L^\infty(\Omega)} \leq C e^{-\sigma_2 t} \quad \text{for all } t > t_2.$$

Proof of Theorem 1.4.2 (ii). Theorem 1.4.2 (ii) is a direct consequence of Lemma 3.3.1 and Lemma 3.3.3. \square

Chapter 4

Spatially heterogeneous time-periodic patterns

We have obtained the global stability of the prey-only steady state $(0, K, \mathbf{0})$ and the coexistence steady state $(u_*, v_*, \mathbf{0})$ under certain parameter conditions (see (3.3.1) for instance). Outside stable parameter regimes, the dynamic of solutions is obscure. In this chapter, we shall first conduct linear analysis to find the parameter regimes such that the constant steady states are unstable, and then perform numerical simulations in these parameter regimes to exhibit possible patterns. Indeed, we observed spatially heterogeneous time-periodic patterns which are consistent with the experimental observations as in [23, 24, 52]. Moreover, our result is significantly different from that of [11] which asserts that the ratio-dependent preytaxis model (1.3.4) admits the existence of non-constant steady state without the acceleration assumption.

4.1 Linear instability analysis

In this section, we shall conduct the linear instability analysis to identify the possible parameter regimes of pattern formation. For the sake of brevity, we shall consider the case of

$$f(v) = 2(1 - v/K) \quad \text{and} \quad F(v/u) = \frac{v}{u+v} \quad (\text{i.e., } m = 1 \text{ in (1.2.5)}). \quad (4.1.1)$$

We start with the corresponding ODE system (noting that $\mathbf{w} \equiv \mathbf{0}$ due to the homogeneous Dirichlet boundary condition of \mathbf{w})

$$\begin{cases} u_t = \alpha u F(v/u) - \mu u, \\ v_t = v f(v) - u F(v/u). \end{cases} \quad (4.1.2)$$

There are three possible equilibria (u_s, v_s) of (4.1.2): $(0, 0)$, $(0, K)$ and (u_*, v_*) , where

$$(u_*, v_*) = \left(\frac{K(\alpha - \mu)}{\alpha}, \frac{K\mu}{\alpha} \right)$$

is given by (1.4.5). Denote \mathbf{J} and J_i ($i = 1, 2, 3, 4$) by

$$\mathbf{J} = \begin{pmatrix} J_1 & J_2 \\ J_3 & J_4 \end{pmatrix} = \begin{pmatrix} \frac{\alpha v_s^2}{(u_s + v_s)^2} - \mu & \frac{\alpha u_s^2}{(u_s + v_s)^2} \\ -\frac{v_s^2}{(u_s + v_s)^2} & 2 - \frac{4v_s}{K} - \frac{u_s^2}{(u_s + v_s)^2} \end{pmatrix}.$$

Then the eigenvalue of \mathbf{J} , denoted by ρ , satisfies

$$\rho^2 - (J_1 + J_4)\rho + J_1 J_4 - J_2 J_3 = 0. \quad (4.1.3)$$

Based on the Routh-Hurwitz criterion (cf. [33, Appendix B]), (u_s, v_s) is linearly stable if and only if

$$-(J_1 + J_4) > 0 \quad \text{and} \quad J_1 J_4 - J_2 J_3 > 0.$$

Obviously, the equilibrium $(0, 0)$ is linearly unstable since the roots of (4.1.3) are $\rho_1 = -\mu$ and $\rho_2 = 2 > 0$. Moreover, it follows from

$$\mathbf{J}|_{(0,K)} = \begin{pmatrix} \alpha - \mu & 0 \\ -1 & -2 \end{pmatrix} \quad \text{and} \quad \mathbf{J}|_{(u_*, v_*)} = \begin{pmatrix} \frac{\mu(\mu - \alpha)}{\alpha} & \frac{(\alpha - \mu)^2}{\alpha} \\ \frac{-\mu^2}{\alpha^2} & -1 - \frac{\mu^2}{\alpha^2} \end{pmatrix}$$

that the steady state $(0, K)$ is linearly unstable (resp. stable) if $\alpha > \mu$ (resp. $\alpha < \mu$) and the homogeneous coexistence steady state (u_*, v_*) is linearly stable when $\alpha > \mu$ since

$$-(J_1 + J_4) = 1 + \frac{\mu(\alpha(\alpha - \mu) + \mu)}{\alpha^2} > 0 \quad \text{and} \quad J_1 J_4 - J_2 J_3 = 1 - \frac{\mu^2}{\alpha^2} > 0.$$

Next we consider the global stability of prey-only and coexistence steady states of the system (1.4.1). For brevity, we take $\Omega = (0, l)$ with $l > 0$, and linearize the system (1.4.1) at the equilibrium $(u_s, v_s, 0)$ to get the linearized system

$$\begin{cases} u_t = d_u u_{xx} - u_s w_x + J_1 u + J_2 v, & x \in (0, l), t > 0, \\ v_t = d_v v_{xx} + J_3 u + J_4 v, & x \in (0, l), t > 0, \\ w_t = d_w w_{xx} + \gamma v_x, & x \in (0, l), t > 0, \\ u_x = v_x = 0, w = 0, & x = 0, l, t > 0, \end{cases} \quad (4.1.4)$$

which has solutions in the form of (cf. [39, Appendix])

$$\begin{cases} u(x, t) = \sum_{k \geq 0} U_k e^{\lambda t} \cos kx, \\ v(x, t) = \sum_{k \geq 0} V_k e^{\lambda t} \cos kx, \\ w(x, t) = \sum_{k \geq 0} W_k e^{\lambda t} \sin kx, \end{cases} \quad (4.1.5)$$

where the constants U_k , V_k and W_k are determined by Fourier expansions of the initial data, $\lambda = \lambda(k)$ (depending on k) is the temporal growth rate and $k = \frac{N\pi}{l}$ is the wave number with the mode $N = 0, 1, 2, \dots$. Substituting (4.1.5) into (4.1.4) and noting that

$$\{1, \cos(\pi x/l), \sin(\pi x/l), \cos(2\pi x/l), \sin(2\pi x/l), \dots\}$$

forms an orthonormal basis for $L^2(0, l)$, we obtain

$$\begin{cases} \lambda U_k + d_u k^2 U_k + k u_s W_k - J_1 U_k - J_2 V_k = 0, & N = 0, 1, 2, 3, \dots, \\ \lambda V_k + d_v k^2 V_k - J_3 U_k - J_4 V_k = 0, & N = 0, 1, 2, 3, \dots, \\ \lambda W_k + d_w k^2 W_k + \gamma k V_k = 0, & N = 1, 2, 3, \dots. \end{cases} \quad (4.1.6)$$

The case of $k = 0$ (i.e., $N = 0$) is corresponding to the ODE system (4.1.2). By the previous analysis, we know that $N = 0$ is a stable mode for the prey-only (resp. coexistence) steady state if $\alpha < \mu$ (resp. $\alpha > \mu$). When $k \neq 0$ (i.e., $N = 1, 2, \dots$),

(4.1.6) implies that λ is the eigenvalue of matrix \mathcal{A} and satisfies

$$\lambda \begin{pmatrix} U_k \\ V_k \\ W_k \end{pmatrix} = \mathcal{A} \begin{pmatrix} U_k \\ V_k \\ W_k \end{pmatrix} \quad \text{with} \quad \mathcal{A} = \begin{pmatrix} -d_u k^2 + J_1 & J_2 & -k u_s \\ J_3 & -d_v k^2 + J_4 & 0 \\ 0 & -k\gamma & -d_w k^2 \end{pmatrix}.$$

One can immediately check that the prey-only steady state $(0, K, 0)$ is linearly stable under the condition $\alpha < \mu$, since

$$\mathcal{A} = \begin{pmatrix} -d_u k^2 + \alpha - \mu & 0 & 0 \\ -1 & -d_v k^2 - 2 & 0 \\ 0 & -\gamma k & -d_w k^2 \end{pmatrix}$$

only has negative eigenvalues for $k \neq 0$ ($N = 1, 2, \dots$). Therefore, the pattern can only arise possibly from the coexistence steady state. In the following, we assume $\alpha > \mu$ and consider the case of the coexistence steady state. Then by tedious discussions of the sign of eigenvalues of the matrix \mathcal{A} (cf. [31, Sec.4] for instance and we omit the details here for brevity), we obtain that the coexistence steady state $\left(\frac{K(\alpha-\mu)}{\alpha}, \frac{K\mu}{\alpha}, 0\right)$ of system (1.4.1) is

$$\begin{cases} \text{linearly stable,} & \gamma < \tilde{\gamma}, \\ \text{marginally stable,} & \gamma = \tilde{\gamma}, \\ \text{linearly unstable,} & \gamma > \tilde{\gamma}, \end{cases} \quad (4.1.7)$$

where

$$\tilde{\gamma} = \inf_{k=\frac{N\pi}{l} \neq 0} \gamma_*(k^2), \quad \gamma_*(k^2) := b_3 k^4 + b_2 k^2 + b_1 + \frac{b_0}{k^2} \quad (4.1.8)$$

and

$$\begin{aligned}
b_3 &= \alpha^3(d_u + d_v)(d_u + d_w)(d_v + d_w), \\
b_2 &= \alpha^3 d_v^2 \mu(\alpha - \mu) + \alpha^2 d_u^2 (\alpha^2 + \mu^2) \\
&\quad + \alpha^2 [\alpha\mu(\alpha - \mu) + \alpha^2 + \mu^2] [2d_u(d_v + d_w) + d_w(2d_v + d_w)], \\
b_1 &= d_u [\alpha^3 \mu(\alpha - \mu) + \alpha\mu(\alpha^3 - \mu^3)] + \alpha^4 + 2\alpha^2 \mu^2 + \mu^4 \\
&\quad + d_v \alpha\mu(\alpha - \mu) (\alpha\mu(\alpha - \mu) + 2\alpha^2 + \alpha\mu + \mu^2) + d_w (\alpha\mu(\alpha - \mu) + \alpha^2 + \mu^2)^2, \\
b_0 &= \mu(\alpha - \mu)(\alpha + \mu) (\alpha\mu(\alpha - \mu) + \alpha^2 + \mu^2),
\end{aligned}$$

are all positive constants.

Remark 4.1.1. In (4.1.7), “linearly stable” means that all eigenvalues of \mathcal{A} have negative real parts for all mode $N \in \{1, 2, \dots\}$; “linearly unstable” denotes that at least one eigenvalue of \mathcal{A} has a positive real part for some mode $N_0 \in \{1, 2, \dots\}$; and “marginally stable” is the case other than the former two cases.

4.2 Spatio-temporal patterns

In this subsection, we shall use numerical simulations to illustrate that the model (1.4.1) can generate spatially heterogeneous time-period patterns which is an expectable mechanism boosting the persistence of predator-prey interactions (cf. [17]). Besides (4.1.1) (which means that $m = 1$), we shall take the value of parameters in all simulations as follows:

$$\alpha = 3, \mu = K = 1 \quad \text{and} \quad d_u = d_v = d_w = 0.1. \quad (4.2.1)$$

The initial data (u_0, v_0, w_0) are taken as a small random perturbation of the coexistence steady state $(u_*, v_*, 0)$ with 1% deviation :

$$(u_0, v_0, w_0) = (u_* + 0.01 \cdot R, v_* + 0.01 \cdot R, 0.01 \cdot R), \quad (4.2.2)$$

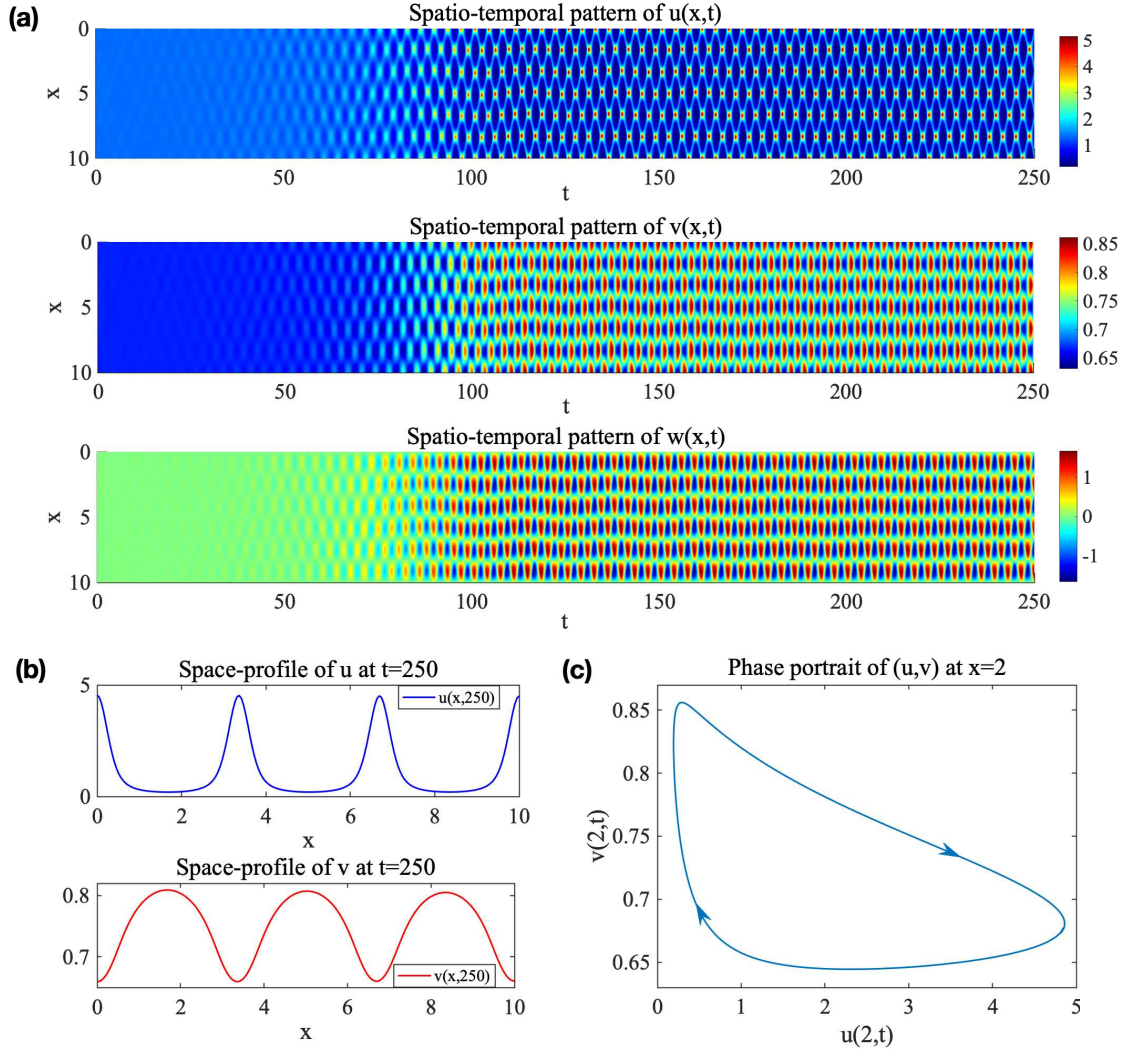


Figure 4.1: Numerical simulation of spatio-temporal patterns generated by (1.4.1) with $\gamma = 15$ in the interval $[0, 10]$, where the initial value (u_0, v_0, w_0) is given by (4.2.2) and other parameter values are chosen as in (4.2.1).

where R is a random variable taking values in $(-1, 1)$ generated by the Matlab and $(u_*, v_*, 0) = (\frac{4}{3}, \frac{2}{3}, 0)$ according to (1.4.5). Recalling the assumption (H), it follows from (4.1.1) that $\delta = 2$ and $f^{-1}(\frac{1}{m}) = f^{-1}(1) = \frac{1}{2} > \frac{\alpha - \mu}{\delta \alpha} = \frac{1}{3}$, which satisfies the condition in Theorem 1.4.2 (ii).

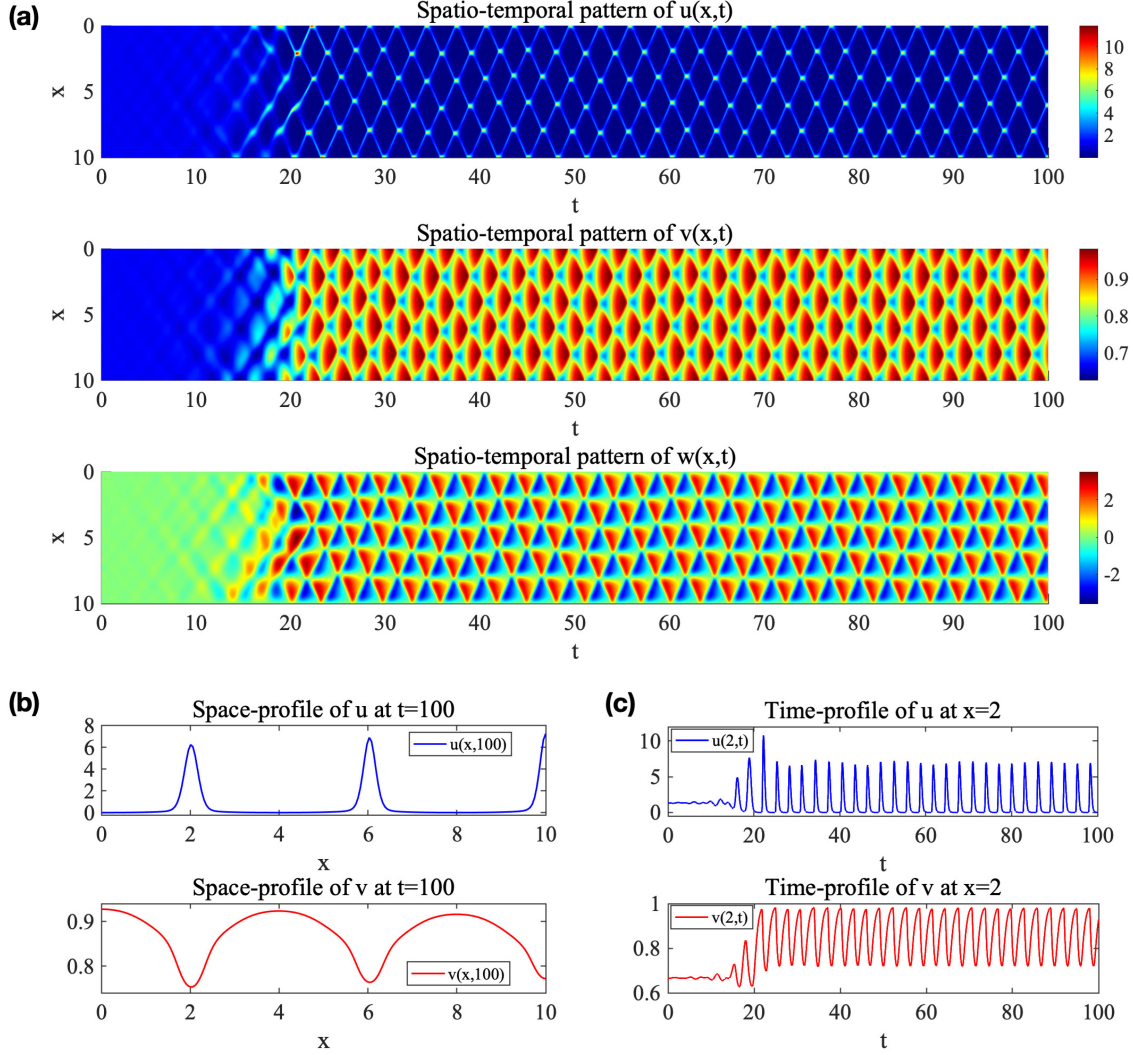


Figure 4.2: Numerical simulation of spatio-temporal patterns generated by (1.4.1) with $\gamma = 30$ in the interval $[0, 10]$, where the initial value (u_0, v_0, w_0) is given by (4.2.2) and other parameter values are chosen as in (4.2.1).

By (4.1.8) we have

$$\begin{aligned} \gamma_*(k^2) \Big|_{k=\frac{N\pi}{10}} &= \left(\frac{27k^4}{500} + \frac{24k^2}{25} + \frac{32}{3k^2} + \frac{82}{15} \right) \Big|_{k=\frac{N\pi}{10}} \\ &= \frac{27\pi^4 N^4}{5000000} + \frac{6\pi^2 N^2}{625} + \frac{3200}{3\pi^2 N^2} + \frac{82}{15} \end{aligned}$$

for $N = 1, 2, 3, \dots$. Moreover, one can check that $\gamma_*(k^2)$ attains its minimum at $k = \frac{5\pi}{10}$ (i.e., $N = 5$) and hence $\tilde{\gamma} = \gamma_*(k^2) \Big|_{k=\frac{5\pi}{10}} \approx 12.4872$.

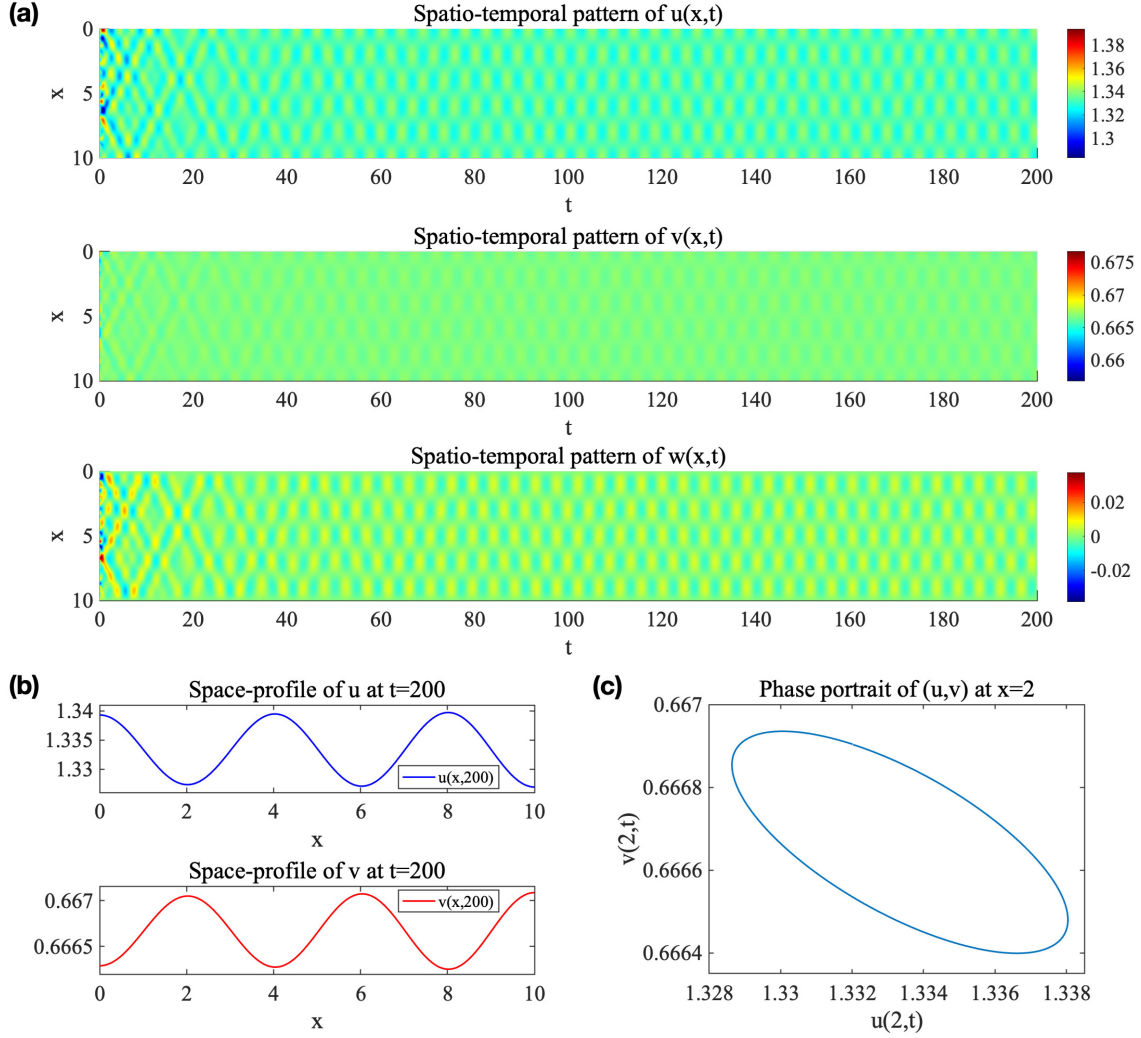


Figure 4.3: Numerical simulation of spatio-temporal patterns generated by (1.4.1) with $\gamma = 12.4872$ in the interval $[0, 10]$, where the initial value (u_0, v_0, w_0) is given by (4.2.2) and other parameter values are chosen as in (4.2.1).

It follows from (4.1.7) that the equilibrium $(\frac{4}{3}, \frac{2}{3}, 0)$ is linearly stable in the subcritical case $\gamma < \tilde{\gamma}$ and can generate patterns in the supercritical case $\gamma > \tilde{\gamma}$. As for the critical case ($\gamma = \tilde{\gamma}$), since the stability of the equilibrium $(\frac{4}{3}, \frac{2}{3}, 0)$ of (1.4.1) is unclear and depends on the specific perturbation, it is interesting to see whether patterns can appear in this case with numerical simulations. Specifically, spatially inhomogeneous time-periodic patterns can generate from the equilibrium $(\frac{4}{3}, \frac{2}{3}, 0)$ with a small perturbation in the supercritical case, such as Fig.4.1 for $\gamma = 15$ and Fig.4.2

for $\gamma = 30$. The two numerical simulations for $\gamma = 15$ and $\gamma = 30$ have three similarities, the first is the similar patterns (see Fig. 4.1-(a) and Fig.4.2-(a)); Second, the predators and prey are segregated heterogeneously in space at a fixed time to achieve coexistence (see Fig.4.1-(b) and Fig.4.2-(b)); the last is that the finally time-periodic of the densities of the predator and the prey at fixed position (see Fig.4.1-(c) for the limit cycle of $(u(2, t), v(2, t))$ and Fig.4.2-(b) for the direct time-periodic profiles of $u(2, t)$ and $v(2, t)$). The difference between these two numerical simulations is that the amplitudes and periodicities of periodic patterns are different. The larger is γ , the larger is the amplitude (compare Fig.4.1-(b) and Fig.4.2-(b)), which indicates that the aggregation effect is stronger with the increase of γ . For the marginally stable case, the similar spatially inhomogeneous time-periodic pattern in the long time is shown in Fig.4.3-(a). However, compare to the former two cases ($\gamma = 15$ and $\gamma = 30$), the obvious difference is that the amplitude of the pattern is eventually very small (see Fig.4.3-(b) and (c)) and retains time-periodic small changes near the equilibrium $(\frac{4}{3}, \frac{2}{3}, 0)$.

It has been shown in [11, Fig.1] that for the conventional ratio-dependent prey-taxis model (1.3.4), non-constant steady states exist in some parameter regimes and no spatially inhomogeneous time-periodic patterns (as the patterns in Fig. 4.1 and Fig. 4.2) arise from the coexistence steady state. From the above analysis for the ratio-dependent preytaxis model (1.4.1) driven by acceleration, we can see that the acceleration assumption brings a significant difference, i.e., spatially inhomogeneous time-periodic patterns arose from the coexistence steady state are observed, which is more suitable to interpret the experimental observations as in [23, 24, 52]. All in all, the ratio-dependent preytaxis model with the acceleration assumption such as (1.4.1) is able to capture different kinds of heterogeneity which are supposed to enhance the persistence of predator-prey interactions with “perfect sharing” (cf. (1.2.5) and [17]). Moreover, our analyses on the model (1.4.1) possibly provide the biological control

some theoretical guidance to inhibit the pest (viewed as the prey in some situations) densities below some economic level as discussed in [39].

Chapter 5

Conclusions and future plans

5.1 Conclusions

This thesis deals with a predator-prey model with a ratio-dependent functional response function and a rational movement assumption – acceleration assumption. The corresponding biological background and motivation are introduced in chapter 1. We have established the global existence and boundedness of classical solutions in chapter 2. Moreover, in chapter 3, the global stability (and also the convergence rates) of the prey-only steady state and the constant coexistence equilibrium are obtained for certain parameter regimes. Outside stable parameter regimes, linear analysis is used to find the unstable parameter regimes and numerical simulations are performed to exhibit that spatially heterogeneous time-periodic patterns will typically arise.

Compared to the conventional ratio-dependent preytaxis model, non-constant steady states exist in some parameter regimes and no spatially inhomogeneous time-periodic patterns arise from the coexistence steady state. However, for our problem, which also takes the acceleration assumption into account, spatially inhomogeneous time-periodic patterns can arise from the coexistence steady state. All in all, the ratio-dependent preytaxis model with the acceleration assumption is able to capture spatial heterogeneity which is supposed to enhance the persistence of predator-prey

interactions. Our results possibly provide biological control with some theoretical guidance to inhibit the pest densities (viewed as the prey in certain situations) below some economic level.

5.2 Future plans

This thesis studied the global dynamic of a one predator one prey preytaxis model. However, in the real world, there are various species and the interactions between them are very complex. Such as a food web system. Therefore, research in this direction is meaningful. From a mathematical point of view, the challenge increases rapidly with the number of species. For instance, even for a three species preytaxis model, there may be three constant coexistence steady states, and the semi-trivial constant coexistence steady states are more than two. Therefore, it can be expected that the dynamic behavior will become extremely complex.

To take a small step in this direction, we may consider one predator and two prey preytaxis model with a ratio-dependent functional response function and the acceleration assumption. Moreover, for the interactions between two prey, we consider the Lotka-Volterra competition. There will be four equations in the considered system. To avoid the model being too complex, we shall only specify the system parameter to certain cases such that there is at most one constant coexistence steady state. In this concrete parameter setting, we study the global dynamics of the model.

Bibliography

- [1] Inkyung Ahn and Changwook Yoon. Global well-posedness and stability analysis of prey-predator model with indirect prey-taxis. *J. Differ. Equ.*, 268(8):4222–4255, 2020.
- [2] Bedr’Eddine Ainseba, Mostafa Bendahmane, and Ahmed Noussair. A reaction-diffusion system modeling predator-prey with prey-taxis. *Nonlinear Anal. Real World Appl.*, 9(5):2086–2105, 2008.
- [3] H. Resit Akcakaya. Population cycles of mammals: evidence for a ratio-dependent predation hypothesis. *Ecol. Monogr.*, 62(1):119–142, 1992.
- [4] H. Resit Akcakaya, Roger Arditi, and Lev R. Ginzburg. Ratio-dependent predation: an abstraction that works. *Ecology*, 76(3):995–1004, 1995.
- [5] Herbert Amann. Dynamic theory of quasilinear parabolic equations. II. Reaction-diffusion systems. *Differ. Integral Equ.*, 3(1):13–75, 1990.
- [6] Herbert Amann. Nonhomogeneous linear and quasilinear elliptic and parabolic boundary value problems. *Teubner-Texte Math.*, 133:9–126, 1993.
- [7] Roger Arditi and Lev R. Ginzburg. Coupling in predator-prey dynamics: ratio-dependence. *J. Theor. Biol.*, 139(3):311–326, 1989.
- [8] Roger Arditi, Lev R. Ginzburg, and H. Resit Akcakaya. Variation in plankton densities among lakes: a case for ratio-dependent predation models. *Amer. Natur.*, 138(5):1287–1296, 1991.
- [9] Roger Arditi, Yu Tyutyunov, Andrey Morgulis, Vasiliy Govorukhin, and Inna Senina. Directed movement of predators and the emergence of density-dependence in predator–prey models. *Theor. Popul. Biol.*, 59(3):207–221, 2001.
- [10] Malay Banerjee. Self-replication of spatial patterns in a ratio-dependent predator-prey model. *Math. Comput. Modelling*, 51(1-2):44–52, 2010.

- [11] Yongli Cai, Qian Cao, and Zhi-An Wang. Asymptotic dynamics and spatial patterns of a ratio-dependent predator–prey system with prey-taxis. *Appl. Anal.*, pages 1–19, 2020.
- [12] Qian Cao, Yongli Cai, and Yong Luo. Nonconstant positive solutions to the ratio-dependent predator-prey system with prey-taxis in one dimension. *Discrete Contin. Dyn. Syst. Ser. S*, 2021.
- [13] Aspriha Chakraborty, Manmohan Singh, David Lucy, and Peter Ridland. Predator-prey model with prey-taxis and diffusion. *Math. Comput. Modelling*, 46(3-4):482–498, 2007.
- [14] Chris Cosner, Donald L. DeAngelis, Jerald S. Ault, and Donald B. Olson. Effects of spatial grouping on the functional response of predators. *Theor. Popul. Biol.*, 56(1):65–75, 1999.
- [15] Yong-Hong Fan and Wan-Tong Li. Global asymptotic stability of a ratio-dependent predator-prey system with diffusion. *J. Comput. Appl. Math.*, 188(2):205–227, 2006.
- [16] Glenn R. Flierl, Daniel Grünbaum, Simon A. Levin, and Donald B. Olson. From individuals to aggregations: the interplay between behavior and physics. *J. Theor. Biol.*, 196(4):397–454, 1999.
- [17] Michael P. Hassell and Roy M. Anderson. Predator–prey and host–pathogen interactions. In *Symposium of the British Ecological Society*, pages 147–196, 1989.
- [18] Xiao He and Sining Zheng. Global boundedness of solutions in a reaction-diffusion system of predator-prey model with prey-taxis. *Appl. Math. Lett.*, 49:73–77, 2015.
- [19] Sze-Bi Hsu, Tzy-Wei Hwang, and Yang Kuang. Global analysis of the Michaelis-Menten-type ratio-dependent predator-prey system. *J. Math. Biol.*, 42(6):489–506, 2001.
- [20] Bei Hu. *Blow-up theories for semilinear parabolic equations*, volume 2018 of *Lecture Notes in Mathematics*. Springer, Heidelberg, 2011.
- [21] Hai-Yang Jin and Zhi-An Wang. Global stability of prey-taxis systems. *J. Differ. Equ.*, 262(3):1257–1290, 2017.

- [22] Hai-Yang Jin and Zhi-An Wang. Global dynamics and spatio-temporal patterns of predator-prey systems with density-dependent motion. *Eur. J. Appl. Math.*, pages 1–31, 2020.
- [23] Peter Kareiva. Experimental and mathematical analyses of herbivore movement: quantifying the influence of plant spacing and quality on foraging discrimination. *Ecol. Monogr.*, 52(3):261–282, 1982.
- [24] Peter Kareiva and Garrett Odell.
- [25] Yang Kuang. Rich dynamics of Gause-type ratio-dependent predator-prey system. *Fields Inst. Commun.*, 21:325–337, 1999.
- [26] Jung M. Lee, Thomas Hillen, and Mark A. Lewis. Continuous traveling waves for prey-taxis. *Bull. Math. Biol.*, 70(3):654–676, 2008.
- [27] Jung M. Lee, Thomas Hillen, and Mark A. Lewis. Pattern formation in prey-taxis systems. *J. Biol. Dyn.*, 3(6):551–573, 2009.
- [28] Chenglin Li, Xuhuang Wang, and Yuanfu Shao. Steady states of a predator-prey model with prey-taxis. *Nonlinear Anal. Theory Methods Appl.*, 97:155–168, 2014.
- [29] Gary M. Lieberman. *Second order parabolic differential equations*. World Scientific Publishing Co., Inc., River Edge, NJ, 1996.
- [30] Demou Luo. Global boundedness of solutions in a reaction-diffusion system of Beddington-DeAngelis-type predator-prey model with nonlinear prey-taxis and random diffusion. *Bound. Value Probl.*, 33 (2018).
- [31] Chunlai Mu, Weirun Tao, and Zhi-An Wang. Global dynamics and spatiotemporal heterogeneity of accelerated preytaxis models. *Preprint*, 2022.
- [32] William W. Murdoch, Cheryl J. Briggs, and Roger M. Nisbet. Consumer-resource dynamics, monographs in population biology. *Princeton University Press*, 36, 2003.
- [33] James D. Murray. *Mathematical Biology I: An introduction*, volume 17 of *Interdisciplinary Applied Mathematics*. Springer-Verlag, New York, third edition, 2002.

- [34] Akira Okubo and Huai C. Chiang. An analysis of the kinematics of swarming of anarete pritchardi kim (diptera: Cecidomyiidae). *Popul. Ecol.*, 16(1):1–42, 1974.
- [35] Akira Okubo, Huai C. Chiang, and Curtis C. Ebbesmeyer. Acceleration field of individual midges, anarete pritchardi (diptera: Cecidomyiidae), within a swarm. *Can. Entomol.*, 109(1):149–156, 1977.
- [36] Peter Y. H. Pang and Mingxin Wang. Qualitative analysis of a ratio-dependent predator-prey system with diffusion. *Proc. Roy. Soc. Edinburgh Sect. A*, 133(4):919–942, 2003.
- [37] Julia K Parrish and Peter Turchin. Individual decisions, traffic rules, and emergent pattern in schooling fish. *Animal groups in three dimensions*, pages 126–142, 1997.
- [38] Feng Rao and Yun Kang. The complex dynamics of a diffusive prey–predator model with an allee effect in prey. *Ecol. Complex.*, 28:123–144, 2016.
- [39] Natalia Sapoukhina, Yuri Tyutyunov, and Roger Arditi. The role of prey taxis in biological control: a spatial theoretical model. *Amer. Natur.*, 162(1):61–76, 2003.
- [40] Yongli Song and Xingfu Zou. Bifurcation analysis of a diffusive ratio-dependent predator-prey model. *Nonlinear Dynam.*, 78(1):49–70, 2014.
- [41] Yongli Song and Xingfu Zou. Spatiotemporal dynamics in a diffusive ratio-dependent predator-prey model near a Hopf-Turing bifurcation point. *Comput. Math. Appl.*, 67(10):1978–1997, 2014.
- [42] Youshan Tao. Global existence of classical solutions to a predator-prey model with nonlinear prey-taxis. *Nonlinear Anal. Real World Appl.*, 11(3):2056–2064, 2010.
- [43] Peter Turchin. Complex population dynamics. *Princeton university press*, 2013.
- [44] Jianping Wang and Mingxin Wang. Boundedness and global stability of the two-predator and one-prey models with nonlinear prey-taxis. *Z. Angew. Math. Phys.*, 69, 63 (2018).
- [45] Jianping Wang and Mingxin Wang. The diffusive Beddington-DeAngelis predator-prey model with nonlinear prey-taxis and free boundary. *Math. Methods Appl. Sci.*, 41(16):6741–6762, 2018.

- [46] Jianping Wang and Mingxin Wang. The dynamics of a predator-prey model with diffusion and indirect prey-taxis. *J. Dynam. Differ. Equ.*, 32(3):1291–1310, 2020.
- [47] Lin Wang. Spatial pattern formation of a ratio-dependent predator prey model. *Chinese Physics B*, 19(9):090206, 2010.
- [48] Mingxin Wang. Note on the Lyapunov functional method. *Appl. Math. Lett.*, 75:102–107, 2018.
- [49] Xiaoli Wang, Wendi Wang, and Guohong Zhang. Global bifurcation of solutions for a predator-prey model with prey-taxis. *Math. Methods Appl. Sci.*, 38(3):431–443, 2015.
- [50] Yuan-Ming Wang. Numerical solutions of a Michaelis-Menten-type ratio-dependent predator-prey system with diffusion. *Appl. Numer. Math.*, 59(5):1075–1093, 2009.
- [51] Zhian Wang and Thomas Hillen. Classical solutions and pattern formation for a volume filling chemotaxis model. *Chaos*, 17(3):037108, 13, 2007.
- [52] Linton Winder, Colin J. Alexander, John M. Holland, Chris Woolley, and Joe N. Perry. Modelling the dynamic spatio-temporal response of predators to transient prey patches in the field. *Ecol. Lett.*, 4(6):568–576, 2001.
- [53] Michael Winkler. Aggregation vs. global diffusive behavior in the higher-dimensional Keller-Segel model. *J. Differ. Equ.*, 248(12):2889–2905, 2010.
- [54] Sainan Wu, Junping Shi, and Boying Wu. Global existence of solutions and uniform persistence of a diffusive predator-prey model with prey-taxis. *J. Differ. Equ.*, 260(7):5847–5874, 2016.
- [55] Tian Xiang. Global dynamics for a diffusive predator-prey model with prey-taxis and classical Lotka-Volterra kinetics. *Nonlinear Anal. Real World Appl.*, 39:278–299, 2018.
- [56] Dongmei Xiao and Leslie Stephen Jennings. Bifurcations of a ratio-dependent predator-prey system with constant rate harvesting. *SIAM J. Appl. Math.*, 65(3):737–753, 2005.